Inorganic Chemistry
Article

Inorg. Chem. **2009**, *48*, 11147–11160 **11147**
DOI: 10.1021/ic901527x

Synthesis of Copper(I) Complexes Containing Enantiopure Pybox Ligands. First Assays on Enantioselective Synthesis of Propargylamines Catalyzed by Isolated Copper(I) Complexes

María Panera,[†] Josefina Díez,[†] Isabel Merino,[‡] Eduardo Rubio,[†,‡] and M. Pilar Gamasa*[,†]

[†]*Departamento de Química Orgánica e Inorgánica, Instituto Universitario de Química Organometálica "Enrique Moles" (Unidad Asociada al C.S.I.C.), Universidad de Oviedo, 33071 Oviedo, Principado de Asturias, Spain, and* [‡]*Unidad de Resonancia Magnética Nuclear, Servicios Científico-Técnicos de la Universidad de Oviedo, 33071 Oviedo, Principado de Asturias, Spain*

Received July 31, 2009

Dinuclear $[Cu_2(R\text{-pybox})_2][X]_2$ [X = PF_6, R-pybox = 2,6-bis[4′-(*S*)-isopropyloxazolin-2′-yl]pyridine (*S*,*S*)-^{i}Pr-pybox (**1**), 2,6-bis[4′-(*R*)-phenyloxazolin-2′-yl]pyridine) (*R*,*R*)-Ph-pybox (**2**), 2,6-bis[4′-(*S*)-isopropyl-5′,5′-difeniloxazolin-2′-yl]pyridine (*S*,*S*)-^{i}Pr-pybox-diPh (**3**); X = OTf, (*R*,*R*)-Ph-pybox (**4**)] and mononuclear complexes $[Cu(R\text{-pybox})_2][PF_6]$ [R-pybox = (*S*,*S*)-^{i}Pr-pybox (**5**), (*R*,*R*)-Ph-pybox (**6**)] have been diastereoselectively prepared by reaction of $[Cu(MeCN)_4][PF_6]$ or CuOTf·0.5C_6H_6 and the corresponding pybox ligand. The reaction of CuX (X = I, Br, Cl) with substituted pybox in a 2:1 molar ratio allows us to synthesize tetranuclear complexes $[Cu_4X_4(R\text{-pybox}\}_2]$ [R-pybox = (*S*,*S*)-^{i}Pr-pybox, X = I (**7**), Br (**8**); (*R*,*R*)-Ph-pybox, X = I (**9**), Br (**10**), Cl (**11**); (*S*,*S*)-^{i}Pr-pybox-diPh, X = I (**12**), Cl (**13**)]. Dinuclear complexes $[Cu_2(\mu\text{-Cl})(R\text{-pybox})_2][CuCl_2]$ [R-pybox = (*S*,*S*)-^{i}Pr-pybox (**15**), (*R*,*R*)-Ph-pybox (**16**)] have been prepared by reaction of CuCl with ^{i}Pr-pybox or Ph-pybox in 3:2 molar ratio. The structures of the complexes **1**, **2**, 7, **15**, **16** and that of the polymeric species $[Cu_4(\mu_3\text{-Br})_3(\mu\text{-Br})(^i\text{Pr-pybox})]_n$ (**14**) have been determined by single-crystal X-ray diffraction analysis. Diffusion studies using ^{1}H and ^{19}F-DOSY experiments provide evidence that the different nuclearity of compounds **1** and **5** is maintained in the solution state and confirm that these ionic compounds exist in solution as stable, discrete, cationic complexes. The complexes **1**−**4**, **6**, **9**, **10**, and **16** as well as the previously reported $[Cu_2\{(S,S)\text{-}^i\text{Pr-pybox}\}_2][OTf]_2$ have been assayed as catalysts in the enantioselective synthesis of propargylamines. The dinuclear complexes $[Cu_2\{(R,R)\text{-Ph-pybox}\}_2][X]_2$ (**2**, **4**) were found to be the most efficient catalysts (up to 89% *e.e.*).

Introduction

Asymmetric synthesis catalyzed by transition-metal complexes bearing enantiopure pybox ligands has received considerable attention in recent years.[1] On the other hand, the structural characterization of novel pybox complexes by X-ray diffraction has become highly interesting and useful[1] because of the information that it provides for gaining insight on the coordination nature of the metal. Most pybox-containing complexes reported so far are mononuclear derivatives wherein the pybox acts generally as tridentate ligand[1] and, in a few cases, as bidentate[2] or monodentate[3] ligand. Moreover, several di- and trinuclear complexes have also been reported: a) Double and triple helical complexes,[4] $[Ag_2\{(S,S)\text{-Bz-pybox}\}_2][BF_4]_2$ and $[Ag_3\{(R,R)\text{-Ph-pybox}\}_3][BF_4]_3$ with bridging pybox ligands, and b) dinuclear rhodium(III) and iridium(III) cationic complexes $[M_2(\mu\text{-Cl})_2(R)_2\{(S,S)\text{-}^i\text{Pr-pybox}\}_2]^{2+}$ (M = Rh, R = Me, (*E*)-CMe=CHPh, $CPh_2=CH_2$; M = Ir, R = Et, HC=$CHCO_2$Me, HC=$CHCO_2$Et) and $[M_2(\mu\text{-Cl})(R)_2Cl_2\{(S,S)\text{-}^i\text{Pr-pybox}\}_2]^+$ (M = Rh, R = Me; M = Ir, R = Et, HC=$CHCO_2$Me, HC=$CHCO_2$Et), containing a tridentate pybox around each rhodium or iridium center.[5,6] In the last years, it has been shown that in situ generated copper(I)/pybox complexes

*To whom correspondence should be addressed. Fax: 34 985103446. E-mail: pgb@uniovi.es.

(1) Desimoni, G.; Faita, G.; Quadrelli, P. *Chem. Rev.* **2003**, *103*, 3119–3154.

(2) (a) Heard, P. J.; Jones, C. *J. Chem. Soc., Dalton Trans.* **1997**, 1083–1091. (b) Heard, P. J.; Tocher, D. A. *J. Chem. Soc., Dalton Trans.* **1998**, 2169–2176.

(3) [Rh{(*S*,*S*)-^{i}Pr-pybox}(CO)L_2][PF_6] (L = phosphine) represents, to the best of our knowledge, the unique example wherein the pybox ligand shows a monodentate coordination: Cuervo, D.; Díez, J.; Gamasa, M. P.; García-Granda, S.; Gimeno, J. *Inorg. Chem.* **2002**, *41*, 4999–5001.

(4) Provent, C.; Hewage, S.; Brand, G.; Bernardinelli, G.; Charbonnière, L. J.; Williams, A. F. *Angew, Chem., Int. Ed.* **1997**, *36*, 1287–1289.

(5) (a) Cuervo, D.; Díez, J.; Gamasa, M. P.; Gimeno, J. *Organometallics* **2005**, *24*, 2224–2232. (b) Cuervo, D.; Gamasa, M. P.; Gimeno, J. *J. Mol. Catal., A* **2006**, *249*, 60–64.

(6) Paredes, P.; Díez, J.; Gamasa, M. P. *J. Organomet. Chem.* **2008**, *693*, 3681–3687.

Published on Web 11/02/2009

catalyze several reactions, e.g., cyclopropanation,[7] azide−alkyne cycloaddition,[8] allylic oxidation,[9] and alkyne addition to imines.[10] The results reported reflect that the efficiency of the process is highly dependent on the type of the pybox ligand as well as on the nature of the copper(I) salt employed, the best results being generally observed with CuOTf·$0.5C_6H_6$ or $[Cu(MeCN)_4]^+$. In spite of that, the participation of a C_2-symmetric tridentate mononuclear complex [Cu(κ^3-*N*,*N*,*N*-pybox)]$^+$ is routinely claimed regardless of the copper precursor used. We report herein our studies focused on: (i) synthesis of mono-, di-, and tetranuclear copper(I) complexes using different copper(I) precursors and various pybox ligands,[11] and (ii) the catalytic activity of isolated copper(I)-pybox complexes in the asymmetric synthesis of propargylamines.

Experimental Section

General Procedures. The reactions were performed under an atmosphere of dry nitrogen using vacuum-line and standard Schlenk techniques. Phenylacetylene, aniline and benzaldehyde were purified by standard methods. All other reagents were obtained from commercial suppliers and used without further purification. Solvents were dried by standard methods and distilled under nitrogen before use. $[Cu(MeCN)_4][PF_6]$, (*S*,*S*)-^{i}Pr-pybox, (*R*,*R*)-Ph-pybox and (*S*,*S*)-^{i}Pr-pybox-diPh were prepared by methods reported in the literature.[12,13] Infrared spectra were recorded on a Perkin-Elmer 1720-XFT spectrometer. The conductivities were measured at room temperature, in acetone or nitromethane solutions (ca. 5×10^{-4} M), with a Jenway PCM3 conductimeter. The C,H,N analyses were carried out with a Perkin-Elmer 240-B microanalyzer (inconsistent analyses were found for complexes **3** and **6** due to incomplete combustion). Electrospray mass spectra (ESI-MS) were recorded on a MicroTof-Q Bruker instrument, operating in the positive mode and using methanol solutions. Mass spectra (MALDI-TOF) were determined with a Microflex Bruker spectrometer, operating in the positive mode; and using dihydroxyanthranol as the matrix. Mass spectra (FAB) were recorded using a VG-AUTOSPEC mass spectrometer (positive mode) using 3-nitrobenzyl alcohol (NBA) as the matrix.

NMR spectra were recorded on a Bruker AV 400 spectrometer operating at 400.13, 100.61, and 161.95 MHz for ^{1}H, ^{13}C and ^{31}P, respectively or on a Bruker AV 300 spectrometer operating at 300.13, 75.48, and 282.40 MHz for ^{1}H, ^{13}C, and ^{19}F, respectively; chemical shifts are reported in ppm and referenced to TMS. DEPT experiments were carried out for all the compounds. Coupling constants *J* are given in hertz. The following atom labels have been used for the ^{1}H and ^{13}C{^{1}H} spectroscopic data of the pybox ligands.

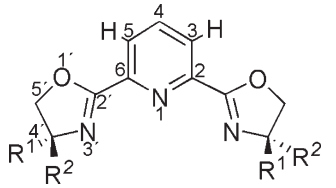

Synthesis of the Dinuclear Complexes $[Cu_2(R\text{-pybox})_2][PF_6]_2$ [R-pybox = (*S*,*S*)-^{i}Pr-pybox (1), (*R*,*R*)-Ph-pybox (2), (*S*,*S*)-^{i}Pr-pybox-diPh (3)]. R-pybox (0.6 mmol) was added to a solution of $[Cu(MeCN)_4][PF_6]$ (0.224 g, 0.6 mmol) in CH_2Cl_2 (25 mL). The resulting solution was stirred for 1 h. Then, the solution was concentrated to ca. 2 mL and diethyl ether (30 mL) (for **1** and **2**) or a mixture of diethyl ether/hexane (2:1) (30 mL) (for **3**) was added. The resulting solid was washed with diethyl ether/hexane (2:1, 3 × 10 mL) and vacuum-dried.

Complex 1. Color: dark-garnet. Yield: 90% (0.275 g). Λ_M = 239 S cm^2 mol^{-1} (acetone, 293 K). IR (KBr): $\nu(PF_6^-)$ 841(f) cm^{-1}. ^{1}H NMR (400.13 MHz, acetone-d_6, 298 K): δ 8.64 (m, 2H, H^4 C_5H_3N), 8.50 (d, J_{HH} = 7.9 Hz, 4H, H^{3,5} C_5H_3N), 5.20 (dd, J_{HH} = 9.9, 9.3 Hz, 4H, OCH_2), 4.84 (dd, J_{HH} = 9.3, 9.0 Hz, 4H, OCH_2), 4.30 (m, 4H, C*H*^{i}Pr), 1.96 (m, 4H, C*H*Me$_2$), 0.83 (t, J_{HH} = 6.6 Hz, 24H, CH*Me*$_2$) ppm. ^{13}C{^{1}H} NMR (75.48 MHz, acetone-d$_6$, 298 K): δ 168.5 (s, OCN), 144.0 (s, C^{2,6} C_5H_3N), 142.8 (s, C^4 C_5H_3N), 128.9 (s, C^{3,5} C_5H_3N), 75.2 (s, OCH_2), 71.0 (s, *C*H^{i}Pr), 32.2 (s, *C*HMe$_2$), 18.2, 17.3 (2*s*, CH*Me*$_2$) ppm. Anal. Calcd for $C_{34}H_{46}Cu_2F_{12}N_6O_4P_2 \cdot CH_2Cl_2$: C, 38.05; H, 4.38; N, 7.61. Found: C, 37.91; H, 4.37; N, 7.65.

Complex 2. Color: brown. Yield: 93% (0.322 g). Λ_M = 170 S cm^2 mol^{-1} (acetone, 293 K). IR (KBr): $\nu(PF_6^-)$ 839 (f) cm^{-1}. MS-FAB: *m*/*z* = 432 ([Cu(Ph-pybox)]$^+$, 100%). ^{1}H NMR (300.13 MHz, acetone-d_6, 298 K): δ 8.52 (t, J_{HH} = 7.7, 2H, H^4 C_5H_3N), 8.33 (d, J_{HH} = 7.7, 4H, H^{3,5} C_5H_3N), 7.22 − 7.12 (m, 20H, Ph), 5.59, 5.37 (2*m*, 2 × 4H, OCH_2), 4.94 (m, 4H, C*H*Ph) ppm. ^{13}C{^{1}H} NMR (75.48 MHz, acetone-d$_6$, 298 K): δ 166.4 (OCN), 142.5 (s, C^{2,6} C_5H_3N), 141.4 (s, C^4 C_5H_3N), 128.9 − 127.1 (Ph, C^{3,5} C_5H_3N), 78.0, 77.0 (2*s*, OCH_2), 68.2, 68.0 (2*s*, *C*HPh) ppm. Anal. Calcd for $C_{46}H_{38}Cu_2F_{12}N_6O_4P_2 \cdot CH_2Cl_2$: C, 45.50; H, 3.25; N, 6.77. Found: C, 45.54; H, 3.34; N, 6.81.

Synthesis of the Dinuclear Complex $[Cu_2(Ph\text{-pybox})_2][OTf]_2$ (4). Ph-pybox (0.3 mmol) was added to a solution of CuOTf·$0.5C_6H_6$ (0.050 g, 0.3 mmol) in CH_2Cl_2 (15 mL) and the resulting solution was stirred for 1 h. The solution was then concentrated to ca. 2 mL and diethyl ether (30 mL) was added. The resulting brown solid was washed with diethyl ether (3 × 10 mL) and vacuum-dried. Yield: 83% (0.144 g). Λ_M = 186 S cm^2 mol^{-1} (acetone, 293 K). IR (KBr): ν(OTf$^-$) 1275 (mf), 1156 (f), 1030 (f) cm^{-1}. MS-FAB: *m*/*z* = 801 ([Cu(Ph-pybox)$_2$]$^+$, 15%), 432 ([Cu(Ph-pybox)]$^+$, 100%). ^{1}H NMR (300.13 MHz, acetone-d_6, 298 K): δ 8.55 (t, J_{HH} = 7.9 Hz, 2H, H^4 C_5H_3N), 8.3 (d, J_{HH} = 7.9 Hz, 4H, H^{3,5} C_5H_3N), 7.20 − 7.13 (m, 20H, Ph), 5.65, 5.37 (2*m*, 2 × 4H, OCH_2), 4.94 (m, 4H, C*H*Ph) ppm. ^{13}C{^{1}H} (100.61 MHz, acetone-d_6, 298 K): δ 167.3 (s, OCN), 144.0 (s, C^{2,6} C_5H_3N), 142.2 (s, C^4 C_5H_3N), 138.2 (s, C^{ipso} Ph), 129.9, 129.6, 129.3, 127.9 (4*s*, Ph, C^{3,5} C_5H_3N), 122.5 (q, J_{CF} = 322 Hz, CF_3SO_3), 76.9 (s, OCH_2), 69.0 (s, *C*HPh) ppm. Anal. Calcd for $C_{48}H_{38}N_6Cu_2F_6O_{10}S_2$: C, 49.53; H, 3.29; N, 7.22. Found: C, 49.35; H, 3.43; N, 7.36.

Synthesis of the Mononuclear Complexes $[Cu(R\text{-pybox})_2][PF_6]$ [R-pybox = (*S*,*S*)-^{i}Pr-pybox (5), (*R*,*R*)-Ph-pybox (6)]. R-pybox (0.6 mmol) was added to a solution of $[Cu(MeCN)_4][PF_6]$ (0.112 g, 0.3 mmol) in CH_2Cl_2 (20 mL) and the resulting solution was stirred for 1 h. The solvent was concentrated to ca. 2 mL and diethyl ether (30 mL) was added. The dark solid formed was washed with diethyl ether (3 × 10 mL) and vacuum-dried.

(7) (a) Datta Gupta, A.; Bhuniya, D.; Singh, V. K. *Tetrahedron* **1994**, *50*, 13725–13730. (b) Müller, P.; Boléa, C. *Helv. Chim. Acta* **2001**, *84*, 1093–1111. (c) Müller, P.; Boléa, C. *Synlett* **2000**, 826–828.

(8) Meng, J.-C.; Fokin, V. V.; Finn, M. G. *Tetrahedron Lett.* **2005**, *46*, 4543–4546.

(9) Ginotra, S. K.; Singh, V. K. *Tetrahedron* **2006**, *62*, 3573 − 3581 and references therein.

(10) (a) Wei, C.; Li, C. J. *J. Am. Chem. Soc.* **2002**, *124*, 5638–5639. (b) Wei, C.; Mague, J. T.; Li, C.-J. *Proc. Natl. Acad. Sci. U.S.A.* **2004**, *101*, 5749–5754. (c) Bisai, A.; Singh, V. K. *Org. Lett.* **2006**, *8*, 2405–2408. (d) First enantioselective synthesis of α-aminopropargylphosphonates: Dodda, R.; Zhao, C.-G. *Tetrahedron Lett.* **2007**, *48*, 4339–4342.

(11) (a) Díez, J.; Gamasa, M. P.; Panera, M. *Inorg. Chem.* **2006**, *45*, 10043–10045. (b) The complex $[Cu_2\{(S,S)$-^{i}Pr-pybox$\}_2][OTf]_2$ has also been characterized: Gelalcha, F. G.; Schulz, M.; Kluge, R.; Sieler, J. *J. Chem. Soc., Dalton Trans.* **2002**, 2517–2521.

(12) Kubas, G. J. *Inorg. Synth.* **1990**, *28*, 68.

(13) (a) Nishiyama, H.; Sakaguchi, H.; Nakamura, T.; Horihata, M.; Kondo, M.; Itoh, K. *Organometallics* **1989**, *8*, 846–848. (b) Nishiyama, H.; Kondo, M.; Nakamura, T.; Itoh, K. *Organometallics* **1991**, *10*, 500–508. (c) Gupta, A. D.; Bhuniya, D.; Singh, V. K. *Tetrahedron* **1994**, *50*, 13725–13730.

Complex 5. Color: dark-garnet. Yield: 51% (0.124 g). Λ_M = 104 S cm^2 mol^{-1} (acetone, 293 K). IR (KBr): $\nu(PF_6^-)$ 843.0 (f) cm^{-1}. MS-MALDI: m/z = 665 ([Cu(*i*Pr-pybox)$_2$]$^+$, 100%). ^{1}H NMR (400.13 MHz, acetone-d_6, 298 K): δ 8.36 (m, 6H, H^{3,4,5} C_5H_3N), 4.66 (t, J_{HH} = 9.0 Hz, 4H, OCH_2), 4.21 (dd, J_{HH} = 9.0, 8.2 Hz, 4H, OCH_2), 4.05 (m, 4H, C*H*^{i}Pr), 1.71 (m, 4H, C*H*Me$_2$), 0.86 (d, J_{HH} = 6.7 Hz, 12H, CH*Me*$_2$), 0.81 (d, J_{HH} = 6.7 Hz, 12H, CH*Me*$_2$) ppm. ^{13}C{^{1}H} NMR (75.48 MHz, acetone-d_6, 298 K): δ 163.1 (OCN), 144.5 (s, C^{2,6} C_5H_3N), 139.3 (s, C^4 C_5H_3N), 126.8 (s, C^{3,5} C_5H_3N), 72.5 (s, OCH_2), 71.8 (s, *C*H^{i}Pr), 32.2 (s, *C*HMe$_2$), 17.7 (s, CH*Me*$_2$) ppm. Anal. Calcd for $C_{34}H_{46}N_6CuF_6O_4P$: C, 50.34; H, 5.72; N, 10.36. Found: C, 49.55; H, 5.54; N, 10.27.

Complex 6. Color: brown. Yield: 65% (0.184 g). Λ_M = 113 S cm^2 mol^{-1} (acetone, 293 K). IR (KBr): $\nu(PF_6^-)$ 841 (f) cm^{-1}. MS-MALDI: m/z = 801 ([Cu(Ph-pybox)$_2$]$^+$, 100%). ^{1}H NMR (300.13 MHz, acetone-d_6, 298 K): δ 8.14 (m, 6H, H^{3,4,5} C_5H_3N), 7.18 (m, 20H, Ph), 5.52, 5.07, 4.31 (3*m*, 3 × 4H, OCH_2, C*H*Ph) ppm. ^{13}C{^{1}H} NMR (75.48 MHz, acetone-d_6, 298 K): δ 164.8 (OCN), 145.2 (s, C^{2,6} C_5H_3N), 141.4 (s, C^{ipso} Ph), 139.9 (s, C^4 C_5H_3N), 129.3, 128.6, 127.9, 127.7 (4*s*, Ph, C^{3,5} C_5H_3N), 77.2 (s, OCH_2), 70.5 (s, *C*HPh) ppm.

Synthesis of the Tetranuclear Complexes [Cu$_4$X$_4$(R-pybox)$_2$] [R-pybox = (*S*,*S*)-^{i}Pr-pybox, X = I (7), Br (8); (*R*,*R*)-Ph-pybox, X = I (9), Br (10), Cl (11); (*S*,*S*)-^{i}Pr-pybox-diPh, X = I (12), Cl (13)]. R-pybox (0.15 mmol) was added to a suspension of CuX (0.3 mmol) in acetone or dichloromethane (15 mL) and the mixture was stirred for 1 h or 3 h (for **12** and **13**). The suspension was then filtered through kieselguhr and the resulting solution was concentrated to ca. 2 mL and diethyl ether (30 mL) was added. The solid was washed with diethyl ether (3 × 10 mL) and vacuum-dried.

Complex 7. Color: dark-orange. Yield: 90% (0.092 g). Λ_M = 87 S cm^2 mol^{-1} (acetone, 293 K); Λ_M = 56 S cm^2 mol^{-1} (nitromethane, 293 K). MS-FAB: m/z = 665 ([Cu(*i*Pr-pybox)$_2$]$^+$, 38%), 556 ([Cu$_2$I(*i*Pr-pybox) + 2]$^+$, 95%), 364 ([Cu(*i*Pr-pybox)]$^+$, 100%). ^{1}H NMR (300.13 MHz, CD_2Cl_2, 298 K): δ 8.21 (m, 4H, H^{3,5} C_5H_3N), 8.12 (m, 2H, H^4 C_5H_3N), 4.71 (m, 8H, OCH_2), 4.53 (m, 4H, C*H*^{i}Pr), 2.42 (m, 4H, C*H*Me$_2$), 0.95 (d, J_{HH} = 6.7 Hz, 12H, CH*Me*$_2$), 0.88 (d, J_{HH} = 6.7 Hz, 12H, CH*Me*$_2$) ppm. ^{13}C{^{1}H} NMR (75.48 MHz, CD_2Cl_2, 298 K): δ 163.1 (s, OCN), 144.8 (s, C^{2,6} C_5H_3N), 139.2 (s, C^4 C_5H_3N), 128.0 (s, C^{3,5} C_5H_3N), 72.5 (s, *C*H^{i}Pr), 71.3 (s, OCH_2), 31.6 (s, *C*HMe$_2$), 19.2, 16.8 (2*s*, CH*Me*$_2$) ppm. Anal. Calcd for $C_{34}H_{46}Cu_4I_4N_6O_4 \cdot C_6H_{14}$: C, 33.12; H, 4.17; N, 5.79. Found: C, 33.35; H, 4.03; N, 5.98.

Complex 8. Color: orange. Yield: 70% (0.072 g). Λ_M = 32 S cm^2 mol^{-1} (acetone, 293 K). MS-ESI: m/z = 665 ([Cu(*i*Pr-pybox)$_2$]$^+$, 79%), 508 ([Cu$_2$Br(*i*Pr-pybox) + 2]$^+$, 97%), 445 ([CuBr(*i*Pr-pybox) + 2]$^+$, 86%), 364 ([Cu(*i*Pr-pybox)]$^+$, 100%). MS-MALDI: m/z = 665 ([Cu(*i*Pr-pybox)$_2$]$^+$, 69%), 508 ([Cu$_2$Br(*i*Pr-pybox) + 2]$^+$, 65%), 445 ([CuBr(*i*Pr-pybox) + 2]$^+$, 41%), 364 ([Cu(*i*Pr-pybox)]$^+$, 100%). ^{1}H NMR (300.13 MHz, acetone-d_6, 298 K): δ 8.45 (m, 2H, H^4 C_5H_3N), 8.35 (m, 4H, H^{3,5} C_5H_3N), 4.96, 4.71 (2*m*, 2 × 4H, OCH_2), 4.52 (m, 4H, C*H*^{i}Pr), 2.32 (m, 4H, C*H*Me$_2$), 1.01, 1.00 (2*d*, J_{HH} = 6.7 Hz, 2 × 12H, CH*Me*$_2$) ppm. ^{13}C{^{1}H} NMR (75.48 MHz, acetone-d_6, 298 K): δ 164.2 (s, OCN), 144.0 (s, C^{2,6} C_5H_3N), 140.5 (s, C^4 C_5H_3N), 127.9 (s, C^{3,5} C_5H_3N), 71.9 (s, O*C*H$_2$), 71.3 (s, *C*H^{i}Pr), 31.3 (s, *C*HMe$_2$), 18.2, 16.4 (2*s*, CH*Me*$_2$) ppm. Anal. Calcd for $C_{34}H_{46}N_6Br_4Cu_4O_4$: C, 34.71; H, 3.94; N, 7.14. Found: C, 34.79; H, 4.12; N: 6.95.

Complex 11. Color: cream. Yield: 61% (0.087 g). MS-ESI: m/z = 801 ([Cu(Ph-pybox)$_2$]$^+$, 41%), 532 ([Cu$_2$Cl(Ph-pybox)+2]$^+$, 46%), 467 ([CuCl(Ph-pybox)]$^+$, 65%), 432 ([Cu(Ph-pybox)]$^+$, 100%). MS-MALDI: m/z = 801 ([Cu(Ph-pybox)$_2$]$^+$, 94%), 532 ([Cu$_2$Cl(Ph-pybox)+2]$^+$, 39%), 467 ([CuCl(Ph-pybox)]$^+$, 100%), 432 ([Cu(Ph-pybox)]$^+$, 33%). ^{1}H NMR (400.13 MHz, acetone-d_6, 298 K): δ 8.37 (t, J_{HH} = 7.8 Hz, 2H, H^4 C_5H_3N), 8.25 (d, J_{HH} = 7.8 Hz, 4H, H^{3,5} C_5H_3N), 7.40 − 7.21 (m, 20H, Ph), 5.78 (m, 4H, C*H*Ph), 5.33, 4.67 (2*m*, 2 × 4H, OCH_2) ppm. ^{13}C{^{1}H} NMR (100.61 MHz, acetone-d_6, 298 K): δ 164.8 (s, OCN), 143.6 (s, C^{2,6} C_5H_3N), 139.7 (s, C^4 C_5H_3N), 139.3 (s, C^{ipso} Ph), 128.4, 128.2, 128.1, 127.3 (4*s*, Ph, C^{3,5} C_5H_3N), 76.5 (s, OCH_2), 70.1 (s, *C*HPh) ppm. Anal. Calcd for $C_{46}H_{38}N_6Cl_4Cu_4O_4$: C, 48.69; H, 3.38; N, 7.41. Found: C, 48.43; H, 3.51; N, 7.46.

Synthesis of the Dinuclear Complexes [Cu$_2$(*μ*-Cl)(R-pybox)$_2$][CuCl$_2$] [R-pybox = (*S*,*S*)-^{i}Pr-pybox (15), (*R*,*R*)-Ph-pybox (16)]. R-pybox (0.33 mmol) was added to a suspension of CuCl (50 mg, 0.5 mmol) in acetone (10 mL). The resulting brown solution was stirred for 1 h. The solution was then concentrated to ca. 2 mL and diethyl ether (30 mL) was added. The brown solid formed was washed with diethyl ether (3 × 10 mL) and vacuum-dried.

Complex 15. Color cream. Yield: 92% (0.137 g). Λ_M = 128 S cm^2 mol^{-1} (acetone, 293 K). MS-FAB: m/z = 665 ([Cu(*i*Pr-pybox)$_2$]$^+$, 43%), 464 ([Cu$_2$Cl(*i*Pr-pybox) +2]$^+$, 100%), 364 ([Cu(*i*Pr-pybox)]$^+$, 92%). ^{1}H NMR (300.13 MHz, acetone-d_6, 298 K): δ 8.39 (m, 6H, H^{3,4,5} C_5H_3N), 4.83, 4.49 (2*m*, 2 × 4H, OCH_2), 4.35 (m, 4H, C*H*^{i}Pr), 1.96 (m, 4H, C*H*Me$_2$), 0.95 (d, J_{HH} = 6.6 Hz, 12H, CH*Me*$_2$), 0.88 (d, J_{HH} = 6.7 Hz, 12H, CH*Me*$_2$) ppm. ^{13}C {^{1}H} NMR (75.48 MHz, acetone-d_6, 298 K): δ 165.5 (s, OCN), 145.8 (s, C^{2,6} C_5H_3N), 141.6 (s, C^4 C_5H_3N), 129.1 (s, C^{3,5} C_5H_3N), 74.0 (s, OCH_2), 66.9 (s, *C*H^{i}Pr), 33.4 (s, *C*HMe$_2$), 19.5, 18.8 (2*s*, CH*Me*$_2$) ppm. Anal. Calcd for $C_{34}H_{46}Cl_3Cu_3N_6O_4$: C, 45.39; H, 5.15; N, 9.34. Found: C, 45.02; H, 5.04; N, 9.24.

Complex 16. Color: cream. Yield: 64% (0.112 g). Λ_M = 157 S cm^2 mol^{-1} (acetone, 293 K). MS-ESI: m/z = 801 ([Cu(Ph-pybox)$_2$]$^+$, 45%), 532 ([Cu$_2$Cl(Ph-pybox) + 2]$^+$, 47%), 467 ([CuCl(Ph-pybox)]$^+$, 53%), 432 ([Cu(Ph-pybox)]$^+$, 100%). MS-MALDI: m/z = 532 ([Cu$_2$Cl(Ph-pybox) + 2]$^+$, 41%), 432 ([Cu(Ph-pybox)]$^+$, 100%). ^{1}H NMR (400.13 MHz, acetone-d_6, 298 K): δ 8.24 (m, 6H, H^{3,4,5} C_5H_3N), 7.44 − 7.10 (m, 20 H, Ph), 5.80 (m, 4H, C*H*Ph), 5.28, 4.53 (2*m*, 2 × 4H, OCH_2) ppm. ^{13}C{^{1}H} NMR (100.61 MHz, acetone-d_6, 298 K): δ 164.2 (s, OCN), 143.7 (s, C^{2,6} C_5H_3N), 139.6 (s, C^{ipso} Ph), 139.2 (s, C^4 C_5H_3N), 128.3, 128.1, 127.4 (3*s*, Ph, C^{3,5} C_5H_3N), 76.3 (s, OCH_2), 70.7 (s, *C*HPh) ppm. Anal. Calcd for $C_{46}H_{38}N_6Cl_3Cu_3O_4$: C, 53.34; H, 3.70; N, 8.11. Found: C, 53.39; H, 3.81; N, 8.22.

X-ray Data. Suitable crystals for X-ray diffraction analysis were obtained by diffusion of diethyl ether into a solution of the complexes **1** or **16** in dichloromethane. The unit cell of the latter contains complex **16** along with dichloromethane and diethyl ether (3:3:1). The diffusion of hexane into a solution of the complex **8** in dichloromethane gave rise to crystals of a polymeric species **14**. The most relevant crystal and refinement data are collected in Table 1.

Data collection for **1** were performed on a Bruker Smart CCD diffractometer using graphiter monocromated Cu−Kα radiation (λ = 1.5418 Å) and a crystal-to-detector distance of 40 mm. The diffraction frames were integrated using the SAINT package[14] and corrected for absorption with SADABS.[15] Data collection for **14** and **16** were performed on a Oxford Diffraction Xcalibur Nova single-crystal diffractometer using Cu−Kα radiation (λ = 1.5418 Å). Images were collected at a 65 mm fixed crystal-detector distance, using the oscillation method, with 1° oscillation and variable exposure time per image (20−80 s). Data collection strategy was calculated with the program CrysAlis Pro CCD.[16] Data reduction and cell refinement were performed with the program CrysAlis Pro RED.[16] An empirical absorption

(14) *SAINT*, version 6.02; Bruker Analytical X-ray Systems: Madison, WI, 2000.

(15) Sheldrick, G. M. *SADABS: Program for Empirical Absorption Correction*: University of Göttingen: Göttingen, Germany, 1996.

(16) *CrysAlisPro CCD, CrysAlisPro RED*; Oxford Diffraction Ltd.: Abingdon, Oxfordshire, U.K., 2008.

Table 1. Crystal Data and Structure Refinement for Complexes **1**, **14**, and **16**

	1	**14**	**16**·CH_2Cl_2·1/3Et_2O
empirical formula	$C_{34}H_{46}Cu_2F_{12}N_6O_4P_2$	$C_{17}H_{23}Br_4Cu_4N_3O_2$	$3C_{46}H_{38}Cl_3Cu_3N_6O_4\cdot 3CH_2Cl_2\cdot C_4H_{10}O$
fw	1019.79	875.18	3436.41
T (K)	100(2)	150(2)	120(2)
wavelength (Å)	1.5418	1.5418	1.5418
cryst syst	monoclinic	orthorhombic	trigonal
space group	$P2_1$	$P2_12_12_1$	$P3_1$
a (Å)	10.1464(1)	10.3289(2)	22.6511(6)
b (Å)	13.0606(1)	10.9546(2)	22.6511(6)
c (Å)	16.5882(1)	20.8896(4)	24.2694(8)
α (deg)	90	90	90
β (deg)	90.587(1)	90	90
γ (deg)	90	90	120
V (Å^3)	2198.12(3)	2363.64(8)	10783.7(5)
Z	2	4	3
ρ_{calcd} (Mg m^{-3})	1.541	2.459	1.587
μ (mm^{-1})	2.731	12.142	4.535
F (000)	1040	1672	5238
cryst size (mm^3)	0.25 × 0.20 × 0.12	0.13 × 0.08 × 0.05	0.2 × 0.03 × 0.03
θ range (deg)	2.66 to 70.59	4.23 to 74.63	2.90 to 73.86
index ranges	$-11 \le h \le 10$ $-15 \le k \le 14$ $-20 \le l \le 19$	$-12 \le h \le 12$ $-13 \le k \le 13$ $-24 \le l \le 25$	$-16 \le h \le 18$ $-14 \le k \le 26$ $-23 \le l \le 29$
no. of reflns collected	11896	27213	26101
no. of independent reflns	6991 [R(int) = 0.0269]	4699 [R(int) = 0.0337]	17042 [R(int) = 0.0767]
completeness to θ_{max} (%)	97.0	99.0	92.0
refinement method	full-matrix least-squares on F^2	full-matrix least-squares on F^2	full-matrix least-squares on F^2
no. of params/restraints	549/1	275/0	1745/565
GOF on F^2	1.075	1.190	1.047
weight function (a, b)	0.1205, 2.0095	0.0288, 5.2027	0.1498, 0
R_1 [$I > 2\sigma(I)$][a]	R_1 = 0.0603, wR_2 = 0.1643	R_1 = 0.0234, wR_2 = 0.0602	R_1 = 0.0881, wR_2 = 0.2240
R (all data)	R_1 = 0.0615, wR_2 = 0.1660	R_1 = 0.0250, wR_2 = 0.0679	R_1 = 0.1312, wR_2 = 0.2558
absolute structure param	0.00(3)	−0.01(2)	0.01(3)
largest diff. peak and hole (e Å^{-3})	1.471 and −1.945	0.492 and −0.884	1.498 and −1.070

[a] $R_1 = \Sigma(|F_o| - |F_c|)/\Sigma|F_o|$; $wR_2 = \{\Sigma[w(F_o^2 - F_c^2)^2]/\Sigma[w(F_o^2)^2]\}^{1/2}$.

correction was applied using the SCALE3 ABSPACK algorithm as implemented in the program CrysAlis Pro RED.[16]

The software package WINGX[17] was used for space group determination, structure solution and refinement. The structures were solved by Patterson interpretation and phase expansion using DIRDIF[18] (for **1** and **14**) or by direct methods using SIR92[19] (for **16**).

Isotropic least-squares refinement on F^2 using SHELXL97[20a] was performed for **1** and **14**. SHELXL97 (Huge Windows version) was employed for the refinement of **16**.[20b] During the final stages of the refinements, all the positional parameters and the anisotropic temperature factors of all the non-H atoms were refined. For **1** and **16** the H atoms were geometrically located and their coordinates were refined riding on their parent atoms. For **14**, the coordinates of H atoms were found from different Fourier maps, and included in a refinement with isotropic parameters. For **1** and **16** the maximum residual electron density is located near to PF_6^- and heavier atoms, respectively. The function minimized was $[\Sigma w(F_o^2 - F_c^2)/\Sigma w(F_o^2)]^{1/2}$ where $w = 1/[\sigma^2(F_o^2) + (aP)^2 + bP]$ (a and b values are collected in Table 1) with $\sigma(F_o^2)$ from counting statistics and $P = (\mathrm{Max}(F_o^2, 0) + 2F_c^2)/3$. Atomic scattering factors were taken from the International Tables for X-ray Crystallography.[21] Geometrical calculations were made with PARST.[22] The crystallographic plots were made with PLATON.[23]

General Procedure for the Enantioselective Addition of Phenylacetylene to *N*-Benzylideneaniline. Dried and deoxygenated CH_2Cl_2 (0.5 mL) was placed in a three-neck Schlenk flask and the mononuclear (0.04 mmol), dinuclear (0.02 mmol) or tetranuclear (0.01 mmol) precatalyst added under a nitrogen atmosphere. Then, deoxygenated *N*-benzylideneaniline (0.4 mmol) and phenylacetylene (0.6 mmol) were added and the mixture stirred for 48 h at room temperature. The resulting propargylamine was purified by chromatography (silica gel, 5:1 hexane/ethyl acetate). The enantiomeric excess was determined by HPLC (Chiralcel OD-H column, 25 × 0.46 cm) using a 98:2 mixture of hexane/isopropanol as eluent (flow rate 0.5 mL/min, t_R = 23 min (*R*) and t_R = 27 min (*S*)). The absolute configuration was assigned on the basis of the literature data.

General Procedure for the One-Pot Enantioselective Reaction of Aldehydes with Aniline and Phenylacetylene. Dried and deoxygenated CH_2Cl_2 (0.5 mL) was placed in a three-neck Schlenk flask and the dinuclear precatalyst (0.02 mmol), deoxygenated aldehyde ArCHO (0.4 mmol), and aniline (0.48 mmol) were sequentially added under a nitrogen atmosphere. The resulting solution was stirred (1.5 h), deoxygenated phenylacetylene (0.6 mmol) added and the mixture stirred for 48 h at room temperature. The propargylamines were purified by chromatography (silica gel, 5:1 hexane/ethyl acetate). The enantiomeric excess was determined by HPLC (Chiralcel OD-H column, 25 × 0.46 cm) using a 98:2 mixture of hexane/isopropanol as eluent ((a) flow rate 0.5 mL/min, Ar = 4-Cl-Ph, t_R = 33 min (*R*) and t_R = 40 min (*S*); (b) flow rate 0.5 mL/min, Ar = 4-Br-Ph, t_R = 35 min (*R*) and t_R = 42 min (*S*); (c) flow rate 0.5 mL/min, Ar = 4-NO_2−Ph, t_R = 23 min (*R*) and t_R = 27 min (*S*); (d) flow rate 0.4 mL/min Ar = 4-OMe-Ph, t_R = 24 min (*R*) and t_R = 27 min (*S*)). The absolute configuration was assigned on the basis of the literature data.

Results and Discussion

Synthesis of the Dinuclear Complexes $[Cu_2(R\text{-pybox})_2][X]_2$ [X = PF_6, R-pybox = (*S*,*S*)-^{i}Pr-pybox (1), (*R*,*R*)-Ph-pybox (2), (*S*,*S*)-^{i}Pr-pybox-diPh (3); X = OTf, (*R*,*R*)-Ph-pybox (4)]. The reaction of equimolecular amounts of

(17) Farrugia, L. J. *J. Appl. Crystallogr.* **1999**, *32*, 837–838.
(18) Beurskens, P. T.; Admiraal, G.; Beurskens, G.; Bosman, W. P.; García-Granda, S.; Gould, R. O.; Smits, J. M. M.; Smykalla, C. *The DIRDIF Program System*; Technical Report of the Crystallographic Laboratory; University of Nijmegen: Nijmegen, The Netherlands, 1999.
(19) Altomare, A.; Cascarano, G.; Giacovazzo, C.; Gualardi, A. *J. Appl. Crystallogr.* **1993**, *26*, 343–350.
(20) (a) Sheldrick, G. M. *SHELXL97: Program for the Refinement of Crystal Structures*; University of Göttingen: Göttingen, Germany, 1997. (b) Sheldrick, G. M. *SHELXL97: Program for the Refinement of Crystal Structures*, Huge Windows Version; University of Göttingen: Göttingen, Germany, 1997.
(21) *International Tables for X-Ray Crystallography*; Kynoch Press: Birminghan, U.K., 1974; Vol. *IV* (present distributor: Kluwer Academic Publishers; Dordrecht, The Netherlands).
(22) Nardelli, M. *Comput. Chem.* **1983**, *7*, 95–98.
(23) Spek, A. L. *PLATON: A Multipurpose Crystallographic Tool*; University of Utrecht, Utrecht, The Netherlands, 2007.

Scheme 1

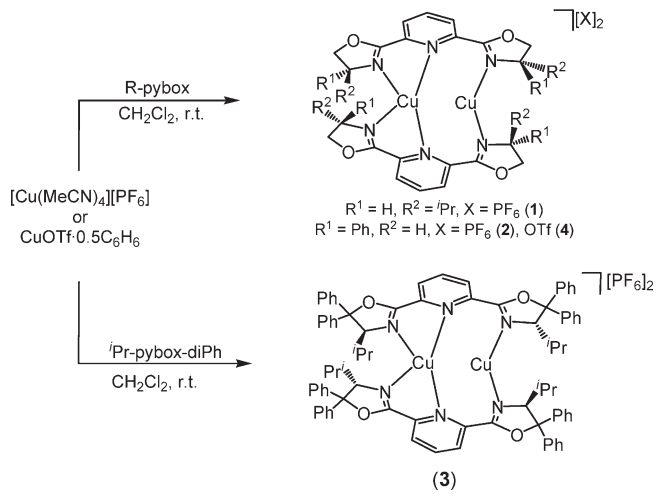

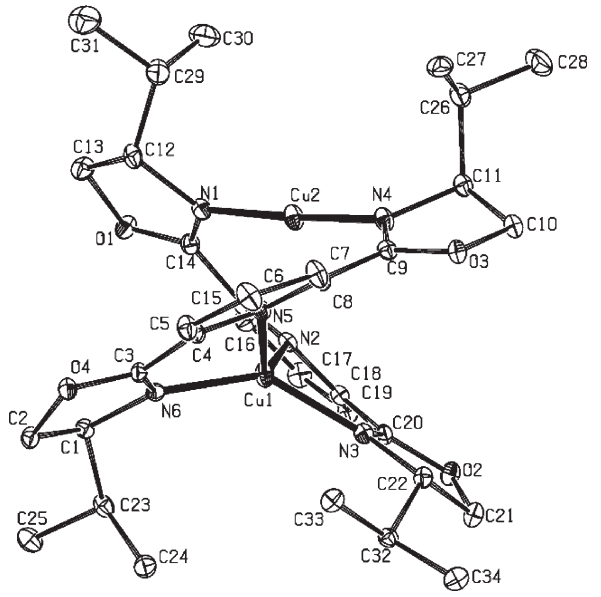

Figure 1. ORTEP drawing of complex **1** showing atom-labeling scheme. Thermal ellipsoids are shown at the 20% probability level. Hydrogen atoms and the PF_6 anions are omitted for clarity.

complex $[Cu(MeCN)_4][PF_6]$ and R-pybox (^{i}Pr-Pybox, Ph-pybox or ^{i}Pr-pybox-diPh) in dichloromethane at room temperature leads to the dinuclear complexes $[Cu_2(R\text{-pybox})_2][PF_6]_2$ [R-pybox = ^{i}Pr-pybox (**1**) (89% yield), Ph-pybox (**2**) (93% yield) and ^{i}Pr-pybox-diPh (**3**) (90% yield)], as single diastereoisomers. The complex $[Cu_2(Ph\text{-pybox})_2][OTf]_2$ (**4**) is analogously prepared (83% yield) using $CuOTf\cdot 0.5C_6H_6$ as the precursor (Scheme 1). All complexes have been characterized by elemental analysis, molar conductivity, mass spectra (**2** − **4**)[24] and NMR spectroscopy (see the Experimental Section). The molar conductivity values found for complexes **1**−**4** (170−217 S cm^2 mol^{-1}) are in the range expected for 1:2 electrolytes.[25] The ^{1}H and ^{13}C resonance signals (298 K) of complexes **1**−**4** in solution are fully consistent with the presence of a C_2 symmetry axis.

The structure of complexes **1** and **2** has been confirmed by single crystal X-ray analyses. ORTEP-type views and selected bonding data of the cation complexes **1** (Figure 1 and Table 2) and **2** (Figure 2) are shown. The structure of complex **1** is analogous to that of the previously reported complex **2**[11a] and shows a dimeric cation $[Cu_2\{(S,S)\text{-}^i\text{Pr-pybox}\}_2]^{2+}$ and two uncoordinated PF_6 anions. The two copper atoms have different co-ordination environments showing linear and distorted tetrahedral arrays. Thus, Cu(2) is coordinated to two oxazoline nitrogens of two different pybox ligands with an N(4)−Cu(2)−N(1) angle of 176.6(2) deg (Figure 1), whereas Cu(1) is bonded to the other oxazoline nitrogen and to both pyridine nitrogens. The Cu(2)−N(1) (1.889(4) Å) and Cu(2)−N(4) (1.884(5) Å) distances are in the range found for other two-coordinate Cu(I) complexes[26] and are shorter than those between the four-coordinate Cu(I) atom and N(2), N(3), N(5), and N(6) atoms. The Cu−Cu distance (2.7292(12) Å) is consistent with nonbonding Cu−Cu contacts.[27] Remarkably, the pybox skeleton is not planar and the two pybox ligands are twisted around the Cu(1)−Cu(2) axis generating a double-helical structure with *P*-helicity.[28] The torsion angles values [N(1)−C(14)−C(15) −N(2) and N(4)−C(9)−C(8)−N(5)] are 23.4(7) and 31.2(8)°, respectively. The cation unit of complex **1** was formed as a single diastereoisomer (*P,S,S*).

Synthesis of the Mononuclear Complexes [Cu(R-pybox)$_2$][PF$_6$] [R-pybox = (*S,S*)-^{i}Pr-pybox (5), (*R,R*)-Ph-pybox (6)]. When the reaction of the complex $[Cu(MeCN)_4][PF_6]$ and R-pybox is carried out in a 1:2 molar ratio (CH_2Cl_2, room temperature), the mononuclear complexes $[Cu(R\text{-pybox})_2][PF_6]$ [R-pybox = (*S,S*)-^{i}Pr-pybox (**5**), (*R,R*)-Ph-pybox (**6**)] are isolated (51 and 65% yield, respectively) (Scheme 2).

Complexes **5** and **6** are presented as mononuclear complexes according with to the mass spectra and conductance measurements in solution. The mass spectra (MALDI) of complexes **5** and **6** show the base peak at m/z 665 ($[Cu(^i\text{Pr-pybox})_2]^+$, 100%) and m/z 801 ($[Cu(\text{Ph-pybox})_2]^+$, 100%), respectively. Unfortunately, an X-ray analysis could not be performed since all attempts to crystallize complexes **5** and **6,** using different mixtures of various solvents, resulted in the formation of complexes **1** and **2**, respectively. A tetrahedral copper environment resulting from bidentate coordination of two pybox ligands, probably through the pyridine nitrogen and an oxazoline nitrogen, is expected for complexes **5** and **6**. However, the room-temperature ^{1}H and ^{13}C NMR spectra are also consistent with the existence of a time averaged structure presenting a C_2 symmetry axis originated by a rapid exchange process that makes both oxazoline groups chemically equivalent.

(24) The mass spectra show an intense peak corresponding to the mass of cation $[Cu(R\text{-pybox})]^+$; the expected $\Delta m/z = 0.5$ peak separations typical of the doubly charged species, $[Cu_2(R\text{-pybox})_2]^{2+}$, are not observed.

(25) Geary, W. J. *Coord. Chem. Rev.* **1971**, *7*, 81–122.

(26) Modder, J. F.; Ernsting, J.-M.; Vrieze, K.; deWit, M.; Stam, C, H.; van Koten, G. *Inorg. Chem.* **1991**, *30*, 1208–1214. (b) Evans, D. A.; Woerpel, K. A.; Scot, M. J. *Angew. Chem., Int. Ed.* **1992**, *104*, 430–432.

(27) (a) Cotton, F. A.; Feng, X.; Matusz, M.; Poli, R. *J. Am. Chem. Soc.* **1988**, *110*, 7077–7083. (b) Cotton, F. A.; Feng, X.; Timmons, D. J. *Inorg. Chem.* **1998**, *37*, 4066–4069.

(28) Classification of helicates: Piguet, C.; Bernardinelli, G.; Hopfgartner, G. *Chem. Rev.* **1997**, *97*, 2005–2062.

Table 2. Selected Bond Distances (Å) and Angles (deg) for Complexes **1**, **14**, and **16**

Complex **1**

bond	distance	bond	distance
Cu(1)−N(2)	2.219(4)	Cu(2)−N(1)	1.889(4)
Cu(1)−N(3)	1.987(4)	Cu(2)−N(4)	1.884(5)
Cu(1)−N(5)	2.272(4)	Cu(1)−Cu(2)	2.7292(12)
Cu(1)−N(6)	1.965(4)		
angle	**value**	**angle**	**value**
N(2)−Cu(1)−N(3)	80.04(16)	N(3)−Cu(1)−N(6)	140.60(17)
N(2)−Cu(1)−N(5)	136.05(15)	N(5)−Cu(1)−N(6)	78.25(16)
N(2)−Cu(1)−N(6)	118.74(16)	N(1)−Cu(2)−N(4)	176.6(2)
N(3)−Cu(1)−N(5)	113.38(16)		

Complex **14**

bond	distance	bond	distance
Cu(1)−N(1)	1.945(4)	Cu(1)−Cu(2)	2.6284(11)
Cu(2)−N(2)	2.373(4)	Cu(3)−Cu(4)	2.9736(13)
Cu(2)−N(3)	1.965(4)		
angle	**value**	**angle**	**value**
N(1)−Cu(1)−Br(1)	104.87(12)	N(2)−Cu(2)−Br(3)	115.16(10)
N(1)−Cu(1)−Br(2)	150.28(12)	N(3)−Cu(2)−Br(2)	104.16(11)
Br(1)−Cu(1)−Br(2)	102.36(3)	N(3)−Cu(2)−Br(3)	137.07(12)
N(2)−Cu(2)−N(3)	77.34(15)	Cu(3)−Br(4)−Cu(4b)	78.21(4)
N(2)−Cu(2)−Br(2)	109.07(10)		

Complex **16**

bond	distance	bond	distance
Cu(1)−N(1)	2.083(12)	Cu(2)−N(4)	2.054(14)
Cu(1)−N(2)	2.234(13)	Cu(2)−N(5)	2.248(13)
Cu(1)−N(6)	1.966(13)	Cu(2)−Cl(1)	2.335(4)
Cu(1)−Cl(1)	2.320(4)	Cu(1)−Cu(2)	2.543(3)
Cu(2)−N(3)	1.940(13)		
angle	**value**	**angle**	**value**
N(1)−Cu(1)−N(2)	78.2(5)	N(3)−Cu(2)−N(4)	109.4(6)
N(1)−Cu(1)−N(6)	108.3(5)	N(3)−Cu(2)−N(5)	120.3(5)
N(2)−Cu(1)−N(6)	116.1(5)	N(4)−Cu(2)−N(5)	78.8(5)
N(1)−Cu(1)−Cl(1)	104.0(4)	N(3)−Cu(2)−Cl(1)	128.3(4)
N(2)−Cu(1)−Cl(1)	101.7(3)	N(4)−Cu(2)−Cl(1)	105.3(4)
N(6)−Cu(1)−Cl(1)	134.0(4)	N(5)−Cu(2)−Cl(1)	103.1(3)
Cu(2)−Cl(1)−Cu(1)	66.23(12)		

Synthesis of the Tetranuclear Complexes [Cu_4X_4(R-pybox}$_2$] [R-pybox = (*S*,*S*)-^{i}Pr-pybox, X = I (7), Br(8); (*R*,*R*)-Ph-pybox, X = I (9), Br (10), Cl (11); (*S*,*S*)-^{i}Pr-pybox-diPh, X = I (12), Cl (13)]. The treatment of a suspension of CuX (X = I, Br, Cl) in acetone or dichloromethane at room temperature with different R-pybox ligands (ca. 2:1 molar ratio) leads to the complexes [Cu_4X_4(R-pybox}$_2$] (**7**−**13**) in 55 − 90% yields after workup (Scheme 3). The resulting complexes have been characterized by elemental analysis, molar conductivity, mass spectra (complexes **8** − **13**) and NMR spectroscopy (see Experimental Section and the Supporting Information for details). Although the structure of complex **7** has been determined by X-ray crystallography, all attempts to grow crystals of **8** resulted in the formation of crystals of a novel polymeric complex **14** (see below).

Structural Determination of the Complex [$Cu_4(\mu_3$-$I)_2(\mu$-$I)_2$(^{i}Pr-pybox)$_2$] (**7**). The structure of complex **7** has been confirmed by a single crystal X-ray analysis. ORTEP-type view of the complex **7** is shown in Figure 3 and selected bonding data are collected in the caption. Complex [Cu_4I_4{(S,S)-^{i}Pr-pybox)$_2$}] (**7**) shows a distorted step structure, a common geometry for complexes with a Cu_4X_4 core,[29] with torsion angle values of −155.97(5)° (Cu(1)−I(2)−Cu(3)−I(4)) and −154.95(5)° (I(1)−Cu(2)−I(3)−Cu(4)). The copper atoms show two different coordination environments. Thus, the terminal copper atoms are coordinated to two iodine atoms and to the oxazoline and pyridine nitrogen atoms of a pybox unit, while the central copper atoms are bonded to three iodine

(29) Hathaway, B. J. In *Comprehensive Coordination Chemistry,* Wilkinson G., Ed.; Pergamon Press: Oxford, U.K., 1987; Vol. *5*, p 557.

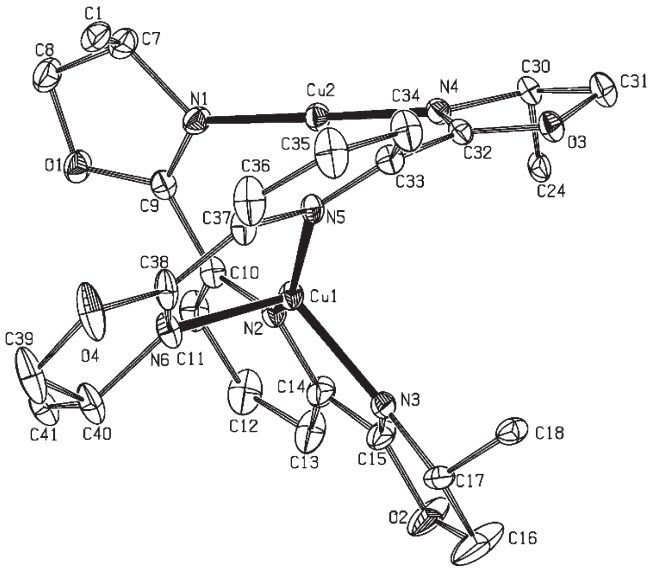

Figure 2. ORTEP drawing of complex **2** showing atom-labeling scheme. Thermal ellipsoids are shown at the 10% probability level. Hydrogen atoms and the PF_6 anions are omitted for clarity and only the C_{ipso} of the phenyl groups are drawn. Selected bond distances (Å) and angles (deg): Cu(1)−Cu(2), 2.6600(13); Cu(1)−N(3), 2.000(6); Cu(1)−N(6), 2.022(6); Cu(1)−N(5), 2.120(6); Cu(1)−N(2), 2.140(6); Cu(2)−N(4), 1.871(5); Cu-(2)−N(1),1.879(6); N(4)−Cu(2)−N(1), 178.9(3).

Scheme 2

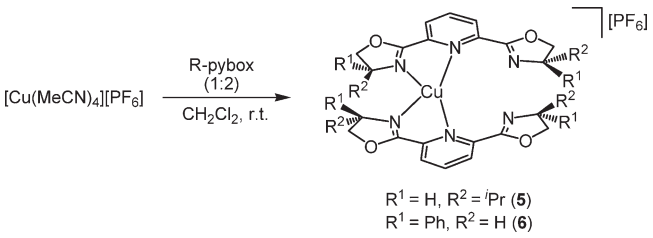

Scheme 3

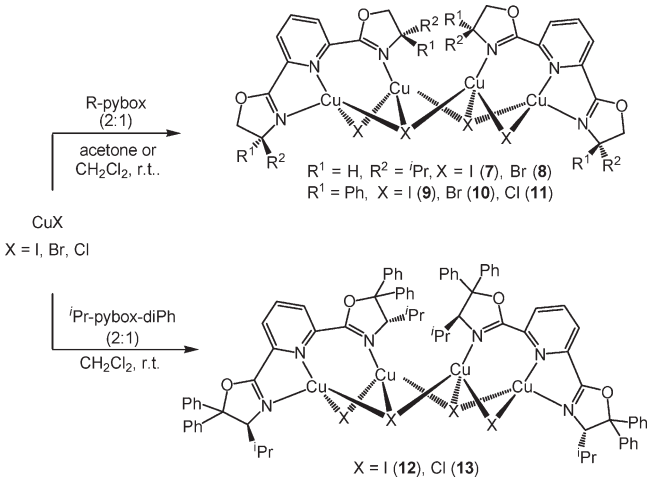

atoms and to the nitrogen of an oxazoline ring. See reference [11a] for further structural data. The structure of complex **7** in solution is different to that found in the solid state as evidenced by diffusion NMR studies (see below) and by the molar conductivity values (1×10^{-4} mol dm^{-3} Me_2CO solution, 293 K, Λ_M = 87 S cm^2 mol^{-1}; 1×10^{-4} mol dm^{-3} CH_3NO_2 solution, 293 K, Λ_M = 56 S cm^2 mol^{-1}). On the other hand, the ^{1}H and ^{13}C NMR resonance signals (298 K) of complex **7** in solution are consistent with a time-averaged C_2 symmetry structure.

Structural Determination of the Complex [$Cu_4(\mu_3$-Br)$_3(\mu$-Br)(^{i}Pr-pybox)]$_n$ (**14**). The ORTEP-type view of the complex **14** is shown in Figure 4 and selected bonding data are collected in Table 2. Complex **14** is a polymeric species in which the repeated unit consists of four copper atoms, four bromine atoms and a (*S,S*)-^{i}Pr-pybox ligand. The copper atoms Cu(1) and Cu(2) are coordinated to ^{i}Pr-pybox and bromine ligands showing a distorted trigonal plane and tetrahedral arrays, respectively. The Cu(1) atom is coordinated to an oxazoline nitrogen N(1) and to Br(1) and Br(2), while Cu(2) is bonded to Br(2) and Br(3) as well as to the pybox ligand through the pyridine N(2) and oxazoline N(3) nitrogens. The copper atoms Cu(3) and Cu(4) are coordinated only to bridging bromine atoms and show slightly distorted tetrahedral and trigonal plane coordination environments. The Cu−Cu bond distances are in the range of 2.6284(11) Å (Cu(1)−Cu(2)) to 3.0235(12) Å (Cu(2)−Cu(4b)).

All attempts to synthesize the polymeric species **14** by using stoichiometric amounts (4:1) of CuBr and ^{i}Pr-pybox and various solvents gave rise to the complex **8** and unreacted CuBr. In the same way, all attempts to crystallize complex **8** have been unsuccessful, even in the presence of ^{i}Pr-pybox that would prevent dissociation.

Synthesis of the Dinuclear Complexes [$Cu_2(\mu$-Cl)(R-pybox)$_2$][$CuCl_2$] [R-pybox = (*S,S*)-^{i}Pr-pybox (15), (*R,R*)-Ph-pybox (16)]. The treatment of CuCl with (*S,S*)-^{i}Pr- and (*R,R*)-Ph-pybox substrates in a 3:2 molar ratio results in the rapid formation of a brown solution from which the complexes [$Cu_2(\mu$-Cl)(^{i}Pr-pybox)$_2$][$CuCl_2$] (**15**) and [Cu_2-(μ-Cl)(Ph-pybox)$_2$][$CuCl_2$] (**16**) are isolated as air stable brown solids in 92% and 64% yield, respectively (Scheme 4). Furthermore, the dinuclear complex **15** is also exclusively formed from a 2:1 CuCl/^{i}Pr-pybox mixture (60% yield).

The structure of complexes **15** and **16** has been confirmed by single-crystal X-ray analyses. ORTEP-type views and selected bonding data of the cation complexes **15** (Figure 5) and **16** (Figure 6 and Table 2) are shown. In analogy with the structure reported for **15**,[11a] the complex **16** consists of a dimeric cation [$Cu_2(\mu$-Cl){(*R,R*)-Ph-pybox}$_2$]$^+$ and an uncoordinated [$CuCl_2$] anion. Each copper atom is bonded to the oxazoline and pyridine nitrogen atoms of a pybox ligand and to the oxazoline nitrogen of the other pybox ligand. The strongly distorted tetrahedral coordination around each copper is completed by one chlorine atom bridge. No significant differences are found between the corresponding distances and angles around each copper. The bond angles around each copper atom are in the range of 78.2(5) to 134.0(4) deg. The pybox skeleton is not planar with torsion angles N(5)−C(33)−C(32)−N(6) and N(2)−C-(14)−C(15)−N(3) of 26(2) and 30(2)°, respectively. Analogously to complexes **1**, **2**, **7**, the Cu−Cu distance (2.543(3) Å) is consistent with nonbonding Cu−Cu contacts.[27]

The ^{1}H and ^{13}C resonance data (298 K) for complexes **15** and **16** in solution are fully consistent with the presence of a C_2 symmetry axis. VT-NMR experiments on

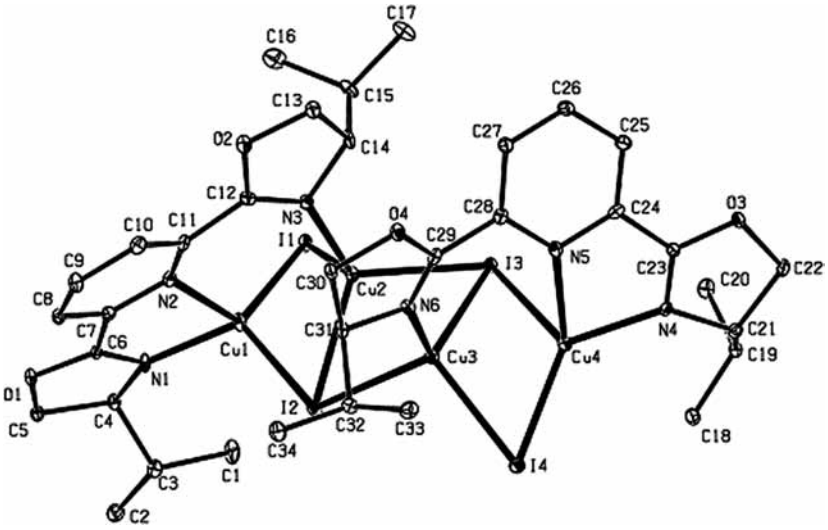

Figure 3. ORTEP drawing of **7** showing atom-labeling scheme. Thermal ellipsoids are shown at the 20% probability level. Hydrogen atoms are omitted for clarity. Selected bond distances (Å): Cu(3)−Cu(4), 2.515(2); Cu(1)−Cu(2), 2.480(2); Cu(2)−Cu(3), 2.742(2); Cu(1)−N(1), 2.018(8); Cu(1)−N(2), 2.277(7); Cu(2)−N(3), 2.031(7); Cu(3)−N(6), 2.037(8); Cu(4)−N(4), 2.017(8); Cu(4)−N(5), 2.283(8); torsion angles (deg): Cu(1)−I(2)−Cu(3)−I(4), −155.97(5); I(1)−Cu(2)−I(3)−Cu(4), −154.95(5).

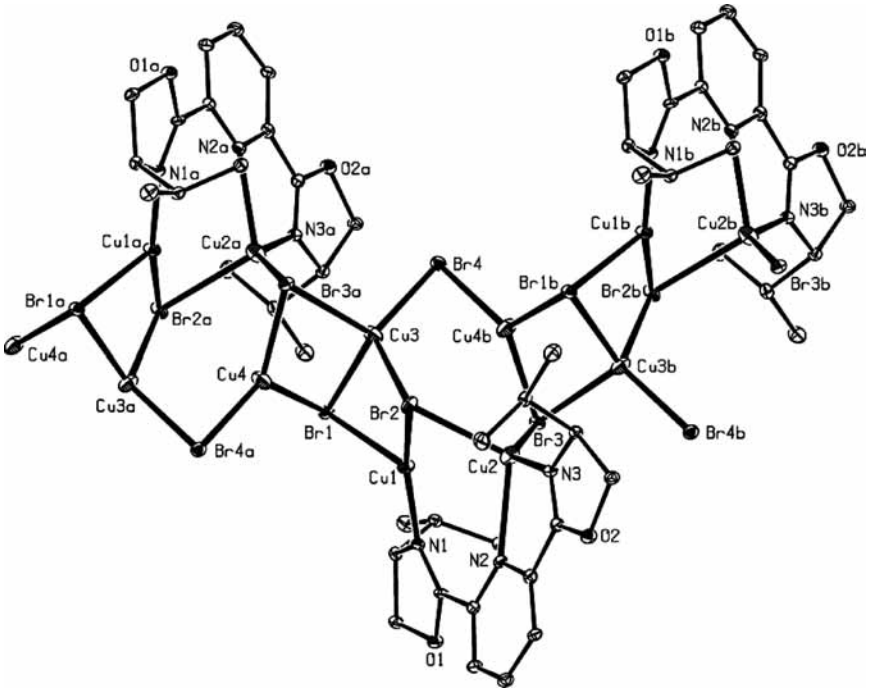

Figure 4. ORTEP drawing of complex **14** showing atom-labeling scheme. Thermal ellipsoids are shown at the 10% probability level. Hydrogen atoms are omitted for clarity.

Scheme 4

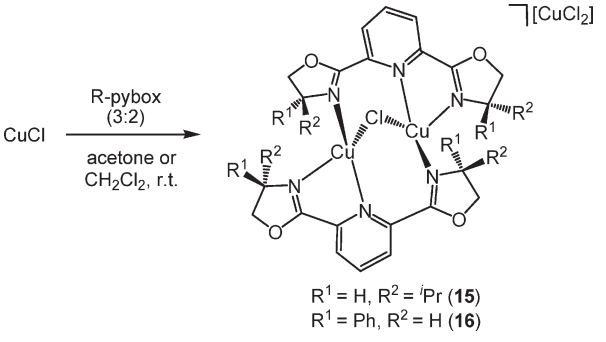

complex **15** reveal that the ^{1}H NMR signals broaden between 213 and 183 K, thus proving the presence of a mixture of several species in solution.

Synthesis of the Dinuclear Complex [Cu_2Cl\{(S,S)-^{i}Pr-pybox)\}$_2$][PF_6] (15a). Complex **1** reacts with excess of NaCl (MeOH, room temperature) affording the complex [$Cu_2(\mu$-Cl)(^{i}Pr-pybox)$_2$][PF_6] (**15a**). The structure of complex **15a** is established on the basis of its mass spectrum, conductivity and ^{1}H and ^{13}C NMR data as well as by comparison with the analogous structure **15** (see Supporting Information).

NMR Elucidation and Diffusion Studies for Complexes 1, 5, and 7. The preliminary NMR study of complexes **1**

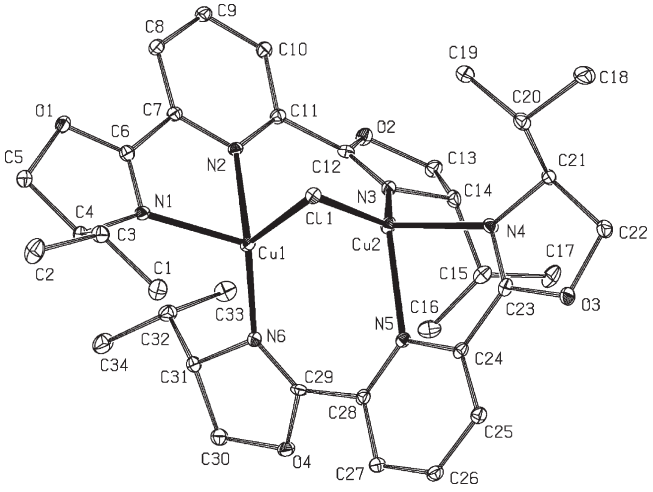

Figure 5. ORTEP drawing of **15** showing atom-labeling scheme. Thermal ellipsoids are shown at the 20% probability level. Hydrogen atoms and $CuCl_2$ anion are omitted for clarity. Selected bond distances (Å) and angles (deg): Cu(1)−Cu(2), 2.6686(9); Cu(1)−Cl(1), 2.3254(12); Cu(2)−Cl(1), 2.3254(12); N(1)−Cu(1), 2.120(4); N(6)−Cu(1), 1.969(4); N(2)−Cu(1), 2.210(4); N(3)−Cu(2), 1.967(4); N(4)−Cu(2), 2.130(4); N(5)−Cu(2), 2.213(4); Cu(1)−Cl(1)−Cu(2), 70.03(3); torsion angles (deg): N(5)−C(28)−C(29)−N(6), −37.0(7); N(2)−C(11)−C(12)−N(3), −36.4(7).

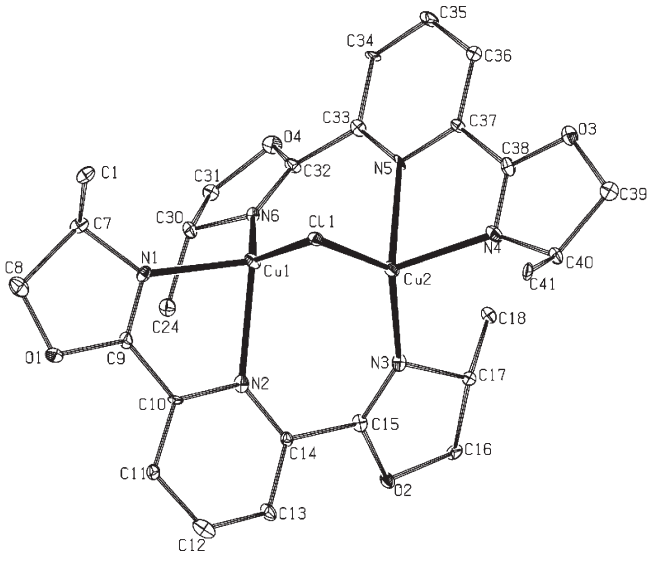

Figure 6. ORTEP drawing of complex **16** showing atom-labeling scheme. Thermal ellipsoids are shown at 20% probability level. Hydrogen atoms and the $CuCl_2$ anion are omitted for clarity and only the C_{ipso}-aryl of the oxazoline groups are drawn.

and **5** showed that their crystalline structures are not maintained in solution, and the room-temperature ^{1}H and ^{13}C NMR spectra of both di- and mononuclear complexes are consistent with a time averaged structure presenting a C_2 symmetry axis. Since the catalytic activity of these complexes takes place in solution, we have carried out several 1D and 2D NMR experiments at room and low temperature on the dinuclear complex **1** and the mononuclear complex **5** to elucidate their structure in the solution state. Additionally, the presence of a potential molecular association/dissociation process, as well as the role of the anion was investigated through diffusion studies.

The ^{1}H and ^{13}C NMR spectra of compound **1** in acetone-d_6 at 298 K show one set of signals for the 4 oxazoline rings as well as for the 2 pyridine rings. This is consistent with a rapid pyridine ligand exchange between the two copper nuclei, producing the observed time-averaged structure with a C_2 symmetry axis. The unique signals at ^{31}P NMR ($\delta = -144.1$ ppm, sept, $^1J_{PF} = 707.8$ Hz) and ^{19}F NMR ($\delta = -72.6$ ppm, d, $^1J_{PF} = 707.8$ Hz) also suggest the same chemical environment for the two PF_6 anions. ^{1}H and ^{31}P NMR spectra in acetone-d_6 of complex **1** remain unaltered from 298 to 181 K. The lack of any splitting of the signals is in accordance with the rapid ligand exchange process proposed above, occurring even at very low temperatures. The analysis of the COSY, HSQCed and HMBC spectra led to the assignment of the signals in the ^{1}H and ^{13}C NMR spectra. Compared to the free pybox ligand, the complexation to the metal produces a strong deshielding in the ^{1}H chemical shifts of the pyridine ($\Delta\delta_{H-4} = 0.62$ and $\Delta\delta_{H-3,5} = 0.31$ ppm) and methylene hydrogen atoms ($\Delta\delta_{H\text{-}5'} = 0.64$ and 0.69 ppm), as well as in the ^{13}C signals assigned to C-4 (pyridine) ($\Delta\delta = 5.6$ ppm) and to C-2′ atoms (oxazoline) ($\Delta\delta = 6.3$ ppm).[11b] Although the dinuclear complex **1** is stable in solution, successive additions of the free pybox ligand to an NMR sample of **1** led to its progressive conversion into the mononuclear complex **5**, as monitored by ^{1}H NMR.

The mass spectrum (MALDI) of mononuclear complex **5** shows the base peak at m/z 665 $[Cu(^i\text{Pr-pybox})_2]^+$, which accounts for the presence of two pybox ligands in the molecule. The ^{1}H and ^{31}C NMR spectra of compound **5** in acetone-d_6 are also consistent with the presence of a C_2 symmetry axis in the cation complex at room and low temperature (298 to 181 K). In this case, the signals are shifted to lower fields compared to the free pybox ligand, though to a lesser extent than in the case of the dinuclear complex **1** (complex **5** vs complex **1**: $\Delta\delta_{C\text{-}4/H\text{-}4}$ (pyridine) = 2.1/0.38 vs 5.6/0.62 ppm; $\Delta\delta_{C\text{-}2'}$ (oxazoline) = 0.9 vs 6.3 ppm).

The pulsed field gradient spin echo (PGSE) methodology[30] is an extremely useful spectroscopic tool to evaluate the molecular size of the molecules in solution. This technique measures the diffusion coefficient (D in Figure 7a) of the molecule in the NMR sample, which can be related to its hydrodynamic radius (r_H) through the Stokes−Einstein equation (Figure 7b). The hydrodynamic radii calculated in this way correlate well with the radii obtained through X-ray analysis,[31] showing the utility of the method for a fast estimation of the molecular size.

The 2D version of the PGSE experiment (DOSY, Diffusion Ordered Spectroscopy)[32] has been successfully applied in the analysis of mixtures,[33] identification of hydrogen bonding,[34]

(30) Johnson, C. S., Jr. *Prog. Nucl. Magn. Reson. Spectrosc.* **1999**, *34*, 203–256.
(31) Valentini, M.; Pregosin, P. S.; Rüegger, H. *Organometallics* **2000**, *19*, 2551–2555.
(32) Morris, K. F.; Johnson, C. S., Jr. *J. Am. Chem. Soc.* **1992**, *114*, 3139–3141.
(33) (a) Barjat, H.; Morris, G. A.; Smart, S.; Swanson, A. G.; Williams, S. C. R. *J. Magn. Reson., Ser. B* **1995**, *108*, 170–172. (b) Kapur, G. S.; Findeisen, M.; Berger, S. *Fuel* **2000**, *79*, 1347–1351. (c) Politi, M.; Groves, P.; Chávez, M. I.; Cañada, F. J.; Jiménez-Barbero, J. *Carbohydr. Res.* **2006**, *341*, 84–89. (d) Allouche, L.; Marquis, A.; Lehn, J.-M. *Chem. Eur. J.* **2006**, *12*, 7520–7525.
(34) (a) Kapur, G. S.; Cabrita, E. J.; Berger, S. *Tetrahedron Lett.* **2000**, *41*, 7181–7185. (b) Cabrita, E. J.; Berger, S. *Magn. Reson. Chem.* **2001**, *39*, S142–S148.

a) $\ln(I/I_0) = -\gamma^2\delta^2 D(\Delta - \delta/3)g^2$

D = Diffusion coefficient
γ = Gyromagnetic ratio
δ = Gradient length
g = Gradient strength
Δ = Diffusion time

b) $D = \frac{K_B T}{6\pi\eta r_H}$

K_B = Boltzmann constant
η = Solvent viscosity
r_H = Hydrodynamic radius

Figure 7. Pulsed field gradient spin−echo (PGSE) technique: (a) Stejskal−Tanner equation, (b) Stokes−Einstein equation.

chemical exchange[35] or molecular complexation.[36] Although the behavior of organometallic compounds in solution has been studied mainly through the one-dimensional PGSE technique,[37,38] DOSY measurements have also been applied for the characterization of organometallic species.[39]

The possibility that the dynamic process present in the dinuclear compound might involve a fast dissociation step between dinuclear and mononuclear complexes ($[Cu_2\{(S,S)\text{-}^i\text{Pr-pybox}\}_2][PF_6]_2$ and 2 $[Cu\{(S,S)\text{-}^i\text{Pr-pybox}\}][PF_6]$), occurring even at 181 K and not detected at the NMR time scale, was investigated through ^{1}H DOSY NMR. Thus, an NMR sample of complex **1** in CD_2Cl_2, using coaxial tubes to avoid a negative influence of convection,[37d] was subjected to several ^{1}H DOSY experiments varying the diffusion time (Δ in Figure 7a) to detect any possible exchange phenomenon.[35b] The experiments were acquired with the *ledbpgp2s* pulse program and the gradient length (δ in Figure 7a) was optimized with the *ledbpgp2s1d* sequence previously. For $\delta = 2$ ms, the same diffusion coefficient was obtained for all the ^{1}H NMR resonances ($D = 8.1 \times 10^{-10}$ m^2/s) in all the measurements with different diffusion times (Δ = 50, 100, 120, 150, and 300 ms). This result supports the structure of complex **1** as a discrete dinuclear molecule and precludes a dissociation process, being the coordination of the metal to the ligand the only observed dynamic process in solution.

To confirm the different nuclearity of complexes **1** and **5** in the solution state, both the dinuclear complex **1** and the mononuclear complex **5** were subjected to ^{1}H, and ^{19}F DOSY NMR experiments. Given the small differences between the molecular weights of the two compounds, the measurements for each complex were carried out in the presence of a reference compound, added to each NMR sample as an internal standard, to establish a comparison between the diffusion coefficients obtained from the same sample conditions. The complex $[Rh\{(S,S)\text{-}^i\text{Pr-pybox}\}(CO)][PF_6]$ (Figure 8) fulfilled the required conditions regarding chemical similarity, molecular size, and stability in solution and was chosen as the reference compound.

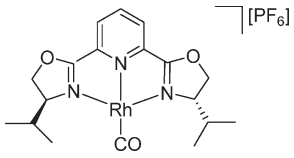

Figure 8. Reference compound $[Rh\{(S,S)\text{-}^i\text{Pr-pybox}\}(CO)][PF_6]$.

Thus, two NMR samples were prepared in coaxial tubes,[37d] using acetone-d_6 as solvent and containing an equimolecular mixture of the [Rh] reference compound and the copper complexes **1** and **5**, respectively. The experiments were performed for both ^{1}H and ^{19}F nuclei and acquired with the *ledbpgp2s* pulse program.[40]

The ^{1}H-DOSY spectra of both mixtures, **1** + [Rh] and **5** + [Rh], are shown in Figure 9. The NMR signals in the chemical shift dimension are resolved in the indirect dimension according to their diffusion coefficient, which results in two well-defined traces for the resonances of each compound. The rhodium complex (MW = 577.26), with a lower molecular weight than the copper complexes **1** (MW = 1019.79) or **5** (MW = 811.28), diffuses faster and exhibits a larger diffusion coefficient (1.41×10^{-9} vs 1.09×10^{-9}m^2/s in the **1** + [Rh] sample or 1.44×10^{-9} vs 1.26×10^{-9}m^2/s in the **5** + [Rh] sample).

The ^{19}F NMR of both NMR samples showed a unique doublet for the two compounds of each mixture at δ = 72.6 ppm ($^1J_{PF} = 707.8$ Hz) that were not either resolved in the diffusion dimension when the ^{19}F DOSY spectra were recorded. The information obtained from the analysis of the DOSY experiments is summarized in Table 3.

Considering that the two molecules in the mixture have a spherical shape, a molecular weight ratio[37c] can be derived from the inverse relation between their diffusion coefficients raised to the power of three ($(D_a/D_b)^3 = (MW_b/MWa)$). As can be observed in Table 3, the ratio of the measured D values in the ^{1}H DOSY spectrum for sample **5** + [Rh] is fully consistent with the ratio of their corresponding molecular weights, which accounts for the presence of the proposed species in solution. The best matching occurs when the comparison is made between the molecular weights of the cationic complexes without considering the PF_6 anions. This observation is supported by the ^{19}F DOSY experiment, that affords a much larger diffusion coefficient for the PF_6 anions (2.29×10^{-9} m^2/s) than the one obtained for the cations ($D = 1.26 \times 10^{-9}$ m^2/s for **5** and $D = 1.44 \times 10^{-9}$ m^2/s for [Rh]), suggesting that the PF_6 anions are moving separately and faster than their cationic complexes.

(35) (a) Cabrita, E. J.; Berger, S.; Bräuer, P.; Kärger, J. *J. Magn. Reson.* **2002**, *157*, 124–131. (b) Cabrita, E. J.; Berger, S. *Magn. Reson. Chem.* **2002**, *40*, S122–S127.

(36) (a) Keresztes, I.; Williard, P. G. *J. Am. Chem. Soc.* **2000**, *122*, 10228–10229. (b) Viel, S.; Mannina, L.; Segre, A. *Tetrahedron Lett.* **2002**, *43*, 2515–2519. (c) Díaz, M. D.; Berger, S. *Carbohydr. Res.* **2000**, *329*, 1–5. (d) Simova, S.; Berger, S. *J. Inclusion Phenom.* **2005**, *53*, 163–170.

(37) Pregosin has shown the great potential that this technique offers of the study of organometallic compounds. See: (a) Valentini, M.; Pregosin, P. S.; Rüegger, H. *Helv. Chim. Acta* **2001**, *84*, 2833–2853. (b) Pregosin, P. S.; Anil Kumar, P. G.; Fernández, I. *Chem. Rev.* **2005**, *105*, 2977–2998. (c) Valentini, M.; Pregosin, P. S.; Rüegger, H. *J. Chem. Soc., Dalton Trans.* **2000**, 4507–4510. (d) Martínez-Viviente, E.; Pregosin, P. S. *Helv. Chim. Acta* **2003**, *86*, 2364–2378. (e) Pregosin, P. S. *Prog. Nucl. Magn. Reson. Spectrosc.* **2006**, *49*, 261–288.

(38) (a) Zuccaccia, C.; Bellachioma, G.; Cardaci, G.; Macchioni, A. *Organometallics* **2000**, *19*, 4663–4665. (b) Macchioni, A.; Ciancaleoni, G.; Zuccaccia, C.; Zuccaccia, D. *Chem. Soc. Rev.* **2008**, *37*, 479–489. (c) Ribas, X.; Dias, J. C.; Morgado, J.; Wurst, K.; Almeida, M.; Parella, T.; Veciana, J.; Rovira, C. *Angew. Chem., Int. Ed.* **2004**, *43*, 4049–4052. (d) Hoefelmeyer, J. D.; Brode, D. L.; Gabbai, F. P. *Organometallics* **2001**, *20*, 5653–5657.

(39) (a) Schlörer, N.; Cabrita, E. J.; Berger, S. *Angew. Chem., Int. Ed.* **2002**, *41*, 107–109. (b) Keresztes, I.; Williar, P. G. *J. Am. Chem. Soc.* **2000**, *122*, 10228–10229.

(40) For the ^{19}F DOSY experiments, the *ledbpgp2s* pulse sequence gave a better signal-to-noise ratio than the *dstebpgp3s* sequence. The diffusion time (Δ, Figure 7a) and the gradient duration (δ, Figure 7a) were optimized with the *ledbpgp2s1d* sequence previously for each measurement until a progressive decay of the signal intensities was obtained to guarantee a good resolution in the diffusion dimension.

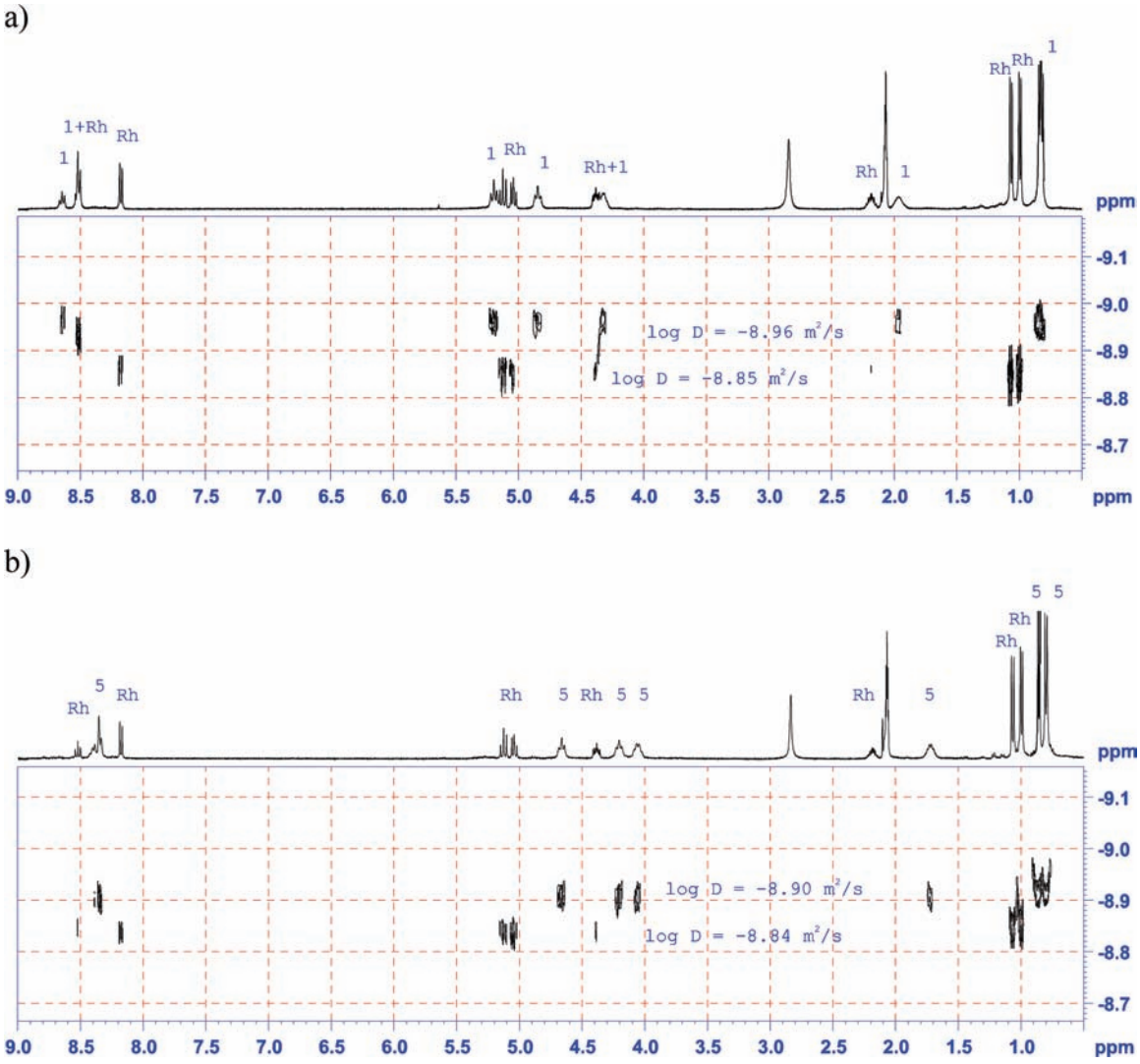

Figure 9. (a) ^{1}H DOSY spectra of sample **1** + [Rh]. (b) ^{1}H DOSY spectra of sample **5** + [Rh].

For the **1** + [Rh] sample, there is also a clear difference between the diffusion coefficients obtained for the cation complexes from ^{1}H-DOSY spectra ($D = 1.09 \times 10^{-9}$ m^2/s for **1** and D = 1.41×10^{-9} m^2/s for [**Rh**]), and those obtained for the PF_6 anions from ^{19}F-DOSY spectra (2.20×10^{-9} m^2/s), what suggests again that they are not diffusing together. The ratio of the measured D values in the ^{1}H DOSY is somehow higher than the expected according to the corresponding molecular weights of the cation complexes (1.29 vs 1.19), which can be indicative of some contribution of the PF_6 anions to the molecular weight of the diffusing cationic species. However, the fact that the about mentioned equivalence ($(D_a/D_b)^3 = (MW_b/MWa)$) may not be accurate for a dinuclear not spherical molecule can not be overlooked.[37c]

To approach the experimental reaction conditions, we also performed the DOSY studies for **1** and **5** in acetone-d_6 and CD_2Cl_2.

The diffusion coefficients obtained for complexes **1** and **5** from the ^{1}H-DOSY and ^{19}F-DOSY experiments, the hydrodynamic radii afforded via the Stokes−Einstein equation (Figure 7b) and the radius calculated from the X-ray structure[41] (only complex **1**) are presented in Table 4. The larger value of the diffusion based radius (3.3 Å) of the PF_6 anion versus its X-ray radius (2.5 Å) supports a small interaction with the cation complex, which can also be detected in the diffusion based radius (6.3 Å) of the cationic fragment, which shows a value halfway between the molecular X-ray radius of complex **1** (6.40 Å) and the cationic fragment radius ($r_{X\text{-ray}}$ = 6.12 Å). When changing the solvent from acetone-d_6 to CD_2Cl_2, the diffusion-based radius of the PF_6 anion for complex **1** noticeably increases (from 3.3 to 6.0 Å) and approaches to the diffusion coefficient of the cationic fragment, that also becomes a bit larger (from 6.3 to 6.6 Å). This observation is in agreement with an increase in the interaction between the ionic fragments when decreasing the polarity of the solvent as previously reported.[37b] Additionally, the ^{1}H^{19}F HOESY spectrum of complex **1** in CD_2Cl_2 solution did not afford any observable ^{1}H−^{19}F cross-peaks, what suggests that the interaction is small and the cation and the anion do not behave as a tight ion-pair.

(41) The X-ray volume ($V_{X\text{-ray}}$) was calculated by dividing the crystallographic unit-cell volume by the number of molecular entities contained in the unit cell, assuming that these have a spherical shape, and subtracting the van der Waals volumes of the counterions: Zhao, Y. H.; Abraham, M. H.; Zissimos, A. M. *J. Org. Chem.* **2003**, *68*, 7368–7373.

Table 3. ^{1}H-DOSY and ^{19}F-DOSY NMR Experiments for NMR Sample Mixtures (**1** + [Rh]) [a] and (**5** + [Rh]) [a]

NMR sample	complex	nucleus	fragment	log D (m^2/s)	D ($\times 10^{-9}$ m^2/s)	D_a/D_b	$(MW_b/MW_a)^{1/3}$
1 + [Rh]	**1**	^{1}H	cation	−8.96	1.09	$D_{Rh}/D_1 = 1.29$	$(MW_1/MW_{Rh})^{1/3} = 1.19$ [b]
1 + [Rh]	[Rh]	^{1}H	cation	−8.85	1.41		
1 + [Rh]	**1**	^{19}F	anion	−8.66	2.20		
1 + [Rh]	[Rh]	^{19}F	anion	−8.66	2.20		
5 + [Rh]	**5**	^{1}H	cation	−8.90	1.26	$D_{Rh}/D_5 = 1.15$	$(MW_5/MW_{Rh})^{1/3} = 1.15$ [c]
5 + [Rh]	[Rh]	^{1}H	cation	−8.84	1.44		
5 + [Rh]	**5**	^{19}F	anion	−8.64	2.29		
5 + [Rh]	[Rh]	^{19}F	anion	−8.64	2.29		

[a] The NMR samples were prepared in a 4 mm NMR tube set inside a 5 mm NMR tube consisting in a mixture of 3 mg of the corresponding copper complex and 3 mg of the rhodium complex in 0.4 mL of acetone-d_6. [b] Molecular weight ratio between the two cations. The molecular weight ratio considering the PF_6 anions is 1.21. [c] Molecular weight ratio between the two cations. The molecular weight ratio considering the PF_6 anions is 1.12.

Table 4. ^{1}H-DOSY and ^{19}F-DOSY NMR Experiments for Compounds **1**[a] and **5**[a]

complex	nucleus	fragment	solvent[b]	log D (m^2/s)	D ($\times 10^{-9}$ m^2/s)	r_H (Å)	$r_{X\text{-ray}}$ (Å)
5	^{1}H	cation	acetone-d_6	−8.90	1.26	5.5	
5	^{19}F	anion	acetone-d_6	−8.60	2.51	2.7	
1	^{1}H	cation	acetone-d_6	−8.96	1.09	6.3	6.40[c]/6.12[d]
1	^{19}F	anion	acetone-d_6	−8.68	2.09	3.3	2.5[e]
1	^{1}H	cation	CD_2Cl_2	−9.10	0.79	6.6	6.40[c]/6.12[d]
1	^{19}F	anion	CD_2Cl_2	−9.06	0.87	6.0	2.5[e]

[a] The NMR samples were prepared in a 4 mm NMR tube set inside a 5 mm NMR tube containing 4.5 mg of the corresponding copper complex in 0.4 mL of acetone-d_6. [b] η (acetone, 298 K) = 0.000316 kg/ms; η (dichloromethane, 298 K) = 0.000414 kg/ms. [c] Molecular radius of the complex **1** calculated from its X-ray structure. [d] Radius of the cation complex obtained from its X-ray structure determined by calculating the volume of complex and subtracting the volume of PF_6^- anions. [e] Radius of the PF_6 anion calculated from its van der Waals volume.

On the other hand, for the mononuclear complex **5** the diffusion based radius of the PF_6 anion (2.7 Å) in acetone-d_6 is closer to the radius of the PF_6 unit, calculated from its van der Waals volume (2.5 Å), than to the radius of the cation (5.5 Å), what accounts for the independent movements of the two ionic fragments previously detected from the data shown in Table 3.

Finally, to check if the solid-state structure of the tetranuclear complex **7** is maintained in solution, we have calculated its hydrodynamic radius and compared to the one obtained from its X-ray analysis. With this aim, an NMR sample of complex **7** was prepared in CD_2Cl_2 and the diffusion coefficient was measured using the same experimental conditions described above (see Table 4, footnote a). The ^{1}H DOSY spectrum afforded a diffusion coefficient $D = 1.0 \times 10^{-9}$ m^2/s (log $D = -9.00$) for compound **7** from which a value of $r_H = 5.27$ Å was obtained for its hydrodynamic radius. On the other hand, the radius for this molecule calculated from its X-ray volume[41] was $r_{X\text{-ray}} = 6.59$ Å. A hypothetical spherical tetranuclear molecule with a hydrodynamic radius $r_H = 6.59$ Å would exhibit a diffusion coefficient $D = 8 \times 10^{-10}$ m^2/s in CD_2Cl_2, as derived from the Stokes−Einstein equation (Figure 7b). The ratio of these diffusion coefficients, ca. 1.25:1, is consistent with the expected ratio for two spherical molecules in which one has twice the volume of the other ($(MWa/MWb)^{1/3} = (2)^{1/3} = 1.26 = (D_b/D_a)$). These data suggest that complex **7** does not maintain its tetranuclear crystalline structure in solution, producing instead a dinuclear structure [Cu_2I_2(*i*Pr-pybox)] or an ionic pair species [(*i*Pr-pybox)$ICu_2\cdots I$] (see conductivities values and FAB spectrum).

Concluding, di- and mononuclear copper(I) complexes containing the (*S,S*)-*i*Pr-pybox ligand **1** and **5** have been characterized in the solution state through NMR experiments. Diffusion ordered spectroscopy has proved that these ionic compounds exist in solution as stable, discrete, dinuclear and mononuclear cationic complexes, respectively. In the case of the dinuclear complex **1** some interaction between the two ionic fragments has been detected, which is not detectable in the mononuclear complex **5**. This NMR technique has also shown that the tetranuclear crystalline structure of the halogenated complex **7** is not maintained in solution.

Enantioselective Synthesis of Propargylamines. Metal-catalyzed enantioselective addition of terminal alkynes to imines and related C=N electrophiles is one of the most convenient methods for the synthesis of optically active propargylamines.[42] The protocols reported for this reaction usually involve the use of a chiral catalyst that is generated in situ by the combination of a copper(I) salt and a suitable chiral ligand.[42,43] In particular, in situ prepared copper(I)−pybox complexes[10a−c,44] have been found useful for this reaction. The first copper-catalyzed enantioselective addition of alkynes to imines was developed by Liu et al., who achieved high yield and

(42) (a) For reviews see: Wei, C.; Li, Z.; Li, C.-J. *Synlett* **2004**, 1472–1483. Zani, L.; Bolm, C. *Chem. Commun.* **2006**, 4263–4275.

(43) Alternative approaches using other metals (e.g., zinc, zirconium) and chiral alkynylborane reagents have been also developed: (a) Zani, L.; Eichhorn, T.; Bolm, C. *Chem. Eur. J.* **2007**, *13*, 2587–2600. (b) Wei, W.; Kobayashi, M.; Ukaji, Y.; Inomata, K. *Chem. Lett.* **2006**, *35*, 176. (c) Traverse, J. F.; Hoveyda, A. H.; Snapper, M. L. *Org. Lett.* **2003**, *5*, 3273–3275. (d) Wu, T. R.; Chong, J. M. *Org. Lett.* **2006**, *8*, 15–18. (e) González, A. Z.; Canales, E.; Soderquist, J. A. *Org. Lett.* **2006**, *8*, 3331–3334.

(44) Polymer-supported pybox: Weissberg, A.; Halak, B.; Portnoy, M. *J. Org. Chem.* **2005**, *70*, 4556–4559. (b) Electrostatically immobilised pybox: McDonagh, C.; O'Conghaile, P.; Gebbink, R. J. M. K.; O'Leary, P. *Tetrahedron Lett.* **2007**, *48*, 4387–4390.

Scheme 5

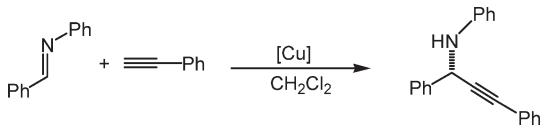

Table 5. Catalytic Activity of Dinuclear Copper(I) Complexes for Enantioselective Synthesis of (1,3-Diphenyl-2-propynyl)aniline[a]

	catalyst	yield (%)[b]	e.e. (%)[c]
1	$[Cu_2(^i\text{Pr-pybox})_2][PF_6]_2$ (**1**)	67	66 (*R*)
2	$[Cu_2(\text{Ph-pybox})_2][PF_6]_2$ (**2**)	65	75 (*S*)
3	$[Cu_2(^i\text{Pr-pybox-diPh})_2][PF_6]_2$ (**3**)	45	34 (*R*)
4	$[Cu_2(^i\text{Pr-pybox})_2][OTf]_2$[11b]	50	68 (*R*)
5	$[Cu_2(\text{Ph-pybox})_2][OTf]_2$ (**4**)	76	83 (*S*)

[a] The reactions were carried out using benzylideneaniline (0.4 mmol). Ratio of benzylideneaniline/phenylacetylene/copper complex = 1:1.5:0.05. The reactions were carried out in anhydrous CH_2Cl_2 (0.5 mL), under a N_2 atmosphere, at room temperature for 48 h. [b] Isolated yield after chromatographic purification. [c] Enantiomeric excess determined by HPLC with a Chiralcel OD-H column. The absolute configuration was assigned on the basis of the literature data.

enantioselectivity by using in situ generated copper(I)−pybox catalysts.[10a] Singh reported a very efficient synthesis of propargylamines using mixtures of $[Cu(MeCN)_4][PF_6]$ or CuOTf·$0.5C_6H_5Me$ and *i*Pr-pybox-diPh.[10c]

Having in mind that in the case of in situ prepared catalysts their catalytic activity is highly dependent on the type of copper salt employed,[8,10a] we have initiated a study of the catalytic activity of isolated Cu(I) complexes. In this context, we have first explored some copper complexes in the addition reaction of phenylacetylene to *N*-benzylideneaniline (Scheme 5).

For comparative purposes, we have first studied the catalytic activity of (*S*,S)-^{i}Pr-pybox, (*S,S*)-^{i}Pr-pybox-diPh and (*R*,*R*)-Ph-pybox copper(I) complexes. Table 5 summarizes the results of this preliminary screening using the dinuclear complexes $[Cu_2(\text{R-pybox})_2][X]_2$. In a typical experiment, a mixture of *N*-benzylideneaniline (0.4 mmol), phenylacetylene (0.6 mmol) and dinuclear copper complex (5 mol %) in CH_2Cl_2 (0.5 mL) is stirred under a N_2 atmosphere at room temperature for 48 h. Although both (*S*,S)-^{i}Pr-pybox and (*R*,*R*)-Ph-pybox complexes are active catalysts, we have observed that the Ph-pybox copper derivatives provide higher enantioselectivity (entries 1 vs 2, 4 vs 5). However, low yield and e.e. are obtained for catalyst **3**, a result that contrasts with the efficiency observed for (*S,S*)-^{i}Pr-diPh/CuOTf mixtures.[10c] (*S*)-Propargylamine is preferentially formed from (*R*,*R*)-Ph-pybox catalysts, whereas (*R*)-propargylamine is the major enantiomer from (*S*,S)-^{i}Pr-pybox catalysts.

The screening of the solvent reveals that other common organic solvents, e.g. toluene, $CHCl_3$, are less efficient in terms of yield and/or enantioselectivity. On the other hand, the reaction rate decreases when more dilute dichloromethane solutions are employed. Finally, the order of sequential addition of benzylideneaniline and phenylacetylene reagents has no influence.

The influence of the nature of the copper complex has been studied using various Ph-pybox complexes of different nuclearity (Table 6). It was found that dinuclear complexes **2** and **4** are much superior to other di- (entry 4), mono- (entry 3), and tetranuclear (entries 5, 6) complexes. Thus, complex **10** provides the product in high chemical yield and low e.e., whereas complexes **9** and **16** are rather ineffective. The results observed (see entries 2 vs 4−6) are in accordance with those reported with in situ prepared catalysts. Good results were achieved for this reaction using catalysts generated from CuOTf, whereas catalysts derived from CuBr and CuCl are less efficient (CuBr/pybox)[10a] or even ineffective (CuCl/bisimine).[45] The unsatisfactory results obtained with CuX-pybox catalysts can be understood in terms of the structure of the complexes **9**, **10**, **16**, which would provide a number of tri or tetrahedral, halogen-containing pybox-copper species in solution (see NMR spectra and X-ray structures); the presence of halides in the coordination sphere of copper apparently decreases the efficiency of the reaction. It should be noted that the complex **6** in which two pybox ligands coordinate to copper in a tetrahedral manner provides very low e.e.; moreover, poor chemical yield is obtained probably because of the coordinative saturation of copper(I) center. ^{1}H NMR experiments for complex **6** in CD_2Cl_2, in the presence of stoichiometric and overstoichiometric amounts of

Table 6. Catalytic Activity of (*R*,*R*)-Ph-pybox Mono-, Di-, and Tetranuclear Copper(I) Complexes for Enantioselective Synthesis of (1,3-Diphenyl-2-propynyl)aniline[a]

	catalyst	yield (%)[b]	e.e. (%)[c]
1	$[Cu_2(\text{Ph-pybox})_2][PF_6]_2$ (**2**)	65	75 (*S*)
2	$[Cu_2(\text{Ph-pybox})_2][OTf]_2$ (**4**)	76	83 (*S*)
3	$[Cu(\text{Ph-pybox})_2][PF_6]$ (**6**)	14	6 (*R*)
4	$[Cu_2(\mu\text{-Cl})(\text{Ph-pybox})_2][CuCl_2]$ (**16**)	16	7 (*R*)
5	$[Cu_4(\mu_3\text{-I})_2(\mu\text{-I})_2(\text{Ph-pybox})_2]$ (**9**)		
6	$[Cu_4(\mu_3\text{-Br})_2(\mu\text{-Br})_2(\text{Ph-pybox})_2]$ (**10**)	89	29 (*R*)

[a] The reactions were carried out using benzylideneaniline (0.4 mmol). Ratio of benzylideneaniline/phenylacetylene/dinuclear copper complex = 1:1.5:0.05. Ratio of benzylideneaniline/phenylacetylene/mononuclear copper complex = 1:1.5:0.1. Ratio of benzylideneaniline/phenylacetylene/tetranuclear copper complex = 1:1.5:0.025. The reactions were carried out in anhydrous CH_2Cl_2 (0.5 mL), under a N_2 atmosphere, at room temperature for 48 h. [b] Isolate yield after chromatographic purification. [c] The enantiomeric excess was determined by HPLC with a Chiralcel OD-H column. The absolute configuration was assigned on the basis of the literature data.

Table 7. Catalytic Activity of (*R*,*R*)-Ph-pybox Dinuclear Copper(I) Complexes for Enantioselective One-Pot, Three-Component Synthesis of Propargylamines[a]

	catalyst	Ar	yield (%)[b]	e.e. (%) (*S*)[c]
1	$[Cu_2(\text{Ph-pybox})_2][PF_6]_2$	PhH	76	77
2	$[Cu_2(\text{Ph-pybox})_2][OTf]_2$	PhH	88	86
3	$[Cu_2(\text{Ph-pybox})_2][PF_6]_2$	4-Cl-Ph	67	82
4	$[Cu_2(\text{Ph-pybox})_2][OTf]_2$	4-Cl-Ph	73	89
5	$[Cu_2(\text{Ph-pybox})_2][OTf]_2$	4-Br-Ph	67	88
6	$[Cu_2(\text{Ph-pybox})_2][OTf]_2$	4-NO_2−Ph	41	77
7	$[Cu_2(\text{Ph-pybox})_2][OTf]_2$	4-MeO-Ph	67	88

[a] Ratio of aldehyde ArCHO/aniline/phenylacetylene/dinuclear copper complex = 1:1.2:1.5:0.05. The reactions were carried out in anhydrous CH_2Cl_2 (0.5 mL), under a N_2 atmosphere, at room temperature for 48 h. [b] Isolated yield after chromatographic purification. [c] The enantiomeric excess was determined by HPLC with a Chiralcel OD-H column. The absolute configuration was assigned on the basis of the literature data.

(45) Colombo, F.; Benaglia, M.; Orlandi, S.; Usuelli, F.; Celentano, G. *J. Org. Chem.* **2006**, *71*, 2064–2070.

Scheme 6

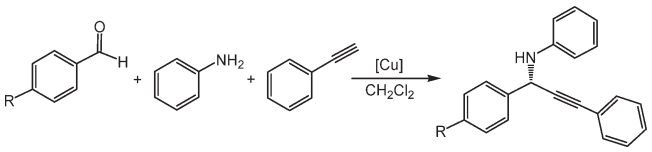

N-benzylideneaniline, have been performed and do not provide evidence of Cu(I)−imine coordination. In spite of the low significance, it is somewhat surprising that the nature of the Ph−pybox complex has influence on the preferential formation of either enantiomer (*S* for complexes **2**, **4** vs *R* for complexes **6**, **10**, **16**).

The reaction was then extended to various imines. We evaluated the efficiency of the most efficient catalyst, $[Cu_2(Ph\text{-}pybox)_2][X]_2$ (X = OTf, PF_6) in the one-pot reaction of several aromatic aldehydes (ArCHO), aniline and phenylacetylene (Scheme 6). Under a nitrogen atmosphere, aniline and the aldehyde in CH_2Cl_2 (0.5 mL) were stirred in the presence of the catalyst during 1.5 h at room temperature. Phenylacetylene was then added and the mixture stirred during 48 h. The results obtained are listed in Table 7.

We have found that the presence of either electron-donating or electron-withdrawing substituents at the para-position of the aldehyde ArCHO has no significant influence on the enantioselectivity (see entries 2, 4, 5, and 7). On the contrary, the effect of the counterion is of importance, the asymmetric induction being generally higher in the case of triflate salts (see entries 1, 3 vs. 2, 4). Finally, moderate-to-high chemical yields are obtained, except in the case of 4-nitrobenzaldehyde (R = NO_2) (entry 6, 41%).

Conclusions

Studies on asymmetric synthesis of propargylamines using isolated copper(I)−pybox complexes are reported for the first time. The results reflect that the efficiency of the reaction is highly dependent on the pybox ligand as well as on the nature of the complexes, with the dinuclear complexes $[Cu_2\{(R,R)\text{-}Ph\text{-}pybox\}_2][X]_2$ (X = OTf, PF_6), obtained from $CuOTf\cdot 0.5C_6H_6$ or $[Cu(MeCN)_4][PF_6]$, being the most efficient catalysts. We tentatively propose complexes $[Cu_2(R\text{-}pybox)_2][X]_2$, containing two equivalent tricoordinate copper centers in the solution state,[46] as the active catalytic species, though mononuclear species resulting from the dissociation of the former during the catalytic cycle cannot be completely excluded. According to ^1H and ^{19}F-DOSY NMR experiments, complexes $[Cu_2(R\text{-}pybox)_2][X]_2$ exist in solution as stable, discrete, dinuclear cationic species.

Moreover, the participation of complexes **9**, **10**, and **16**, which would originate a number of halogen-containing pybox-copper species in solution, would explain the low efficiency in the case of CuX−pybox catalysts. We believe that these findings can provide insight into the real nature of the active copper-pybox catalytic species. Such a catalyst structure is presently almost unknown, though the synthetic impact of the process in terms of conversion and chiral induction is well documented.

Acknowledgment. This work was supported by the Ministerio de Educación y Ciencia of Spain (BQU2003-00255) and Consolider Ingenio 2010 (CSD2007-00006).

Supporting Information Available: The full characterization of complexes **3**, **9**, **10**, **12**, and **13**, as well as the synthesis and characterization of complex **15a**. Experimental conditions for NMR experiments. Crystallographic data for complexes **1**, **14**, and **16** (PDF). This material is available free of charge via the Internet http://pubs.acs.org.

(46) The ^1H NMR spectra of complex **2** in the presence of stoichiometric (1:2) and overstoichiometric amounts of *N*-benzylideneaniline or complex **2**/phenylacetylene (1:2) in CD_2Cl_2 do not provide evidence of Cu(I)−imine or Cu(I)−alkyne coordination.